

AD-A100 343 CHICAGO UNIV IL JAMES FRANCK INST  
THERMAL DESORPTION OF XE FROM THE (110) PLANE OF TUNGSTEN.(U)  
JUN 81 R OPILA, R GOMER

F/G 7/4  
N00014-77-C-0018  
NL

UNCLASSIFIED 7

1 of 1  
AD  
A100-343

END  
DATE  
FILED  
7-8-81  
DTIC

AD A100343

Unclassified

SECURITY CLASSIFICATION OF THIS PAGE (When Data Entered)

REPORT DOCUMENTATION PAGE		READ INSTRUCTIONS BEFORE COMPLETING FORM
1. REPORT NUMBER <i>14)</i>	2. GOVT ACCESSION NO. <i>AD-900 343</i>	3. RECIPIENT'S CATALOG NUMBER <i>II</i>
4. TITLE (and Subtitle) <i>6 Thermal Desorption of Xe from the (110) Plane of Tungsten.</i>		5. TYPE OF REPORT & PERIOD COVERED <i>9, Technical Rept.,</i>
7. AUTHOR(s) <i>10) R. Opila and R. Gomer</i>		8. CONTRACT OR GRANT NUMBER(s) <i>15 ONR N00014-77-C-0018</i>
9. PERFORMING ORGANIZATION NAME AND ADDRESS James Franck Institute University of Chicago Chicago, Illinois 60637		10. PROGRAM ELEMENT, PROJECT, TASK AREA & WORK UNIT NUMBERS <i>12</i>
11. CONTROLLING OFFICE NAME AND ADDRESS Office of Naval Research Physics Program (Code 421) Arlington, Virginia 22217		12. REPORT DATE <i>11 June 1981</i>
14. MONITORING AGENCY NAME & ADDRESS (if different from Controlling Office)		13. NUMBER OF PAGES <i>15</i>
		15. SECURITY CLASS. (of this report) <i>Unclassified</i>
		15a. DECLASSIFICATION/DOWNGRADING SCHEDULE
16. DISTRIBUTION STATEMENT (of this Report)  Approved for public release; distribution unlimited		
17. DISTRIBUTION STATEMENT (of the abstract entered in Block 20, if different from Report)		
18. SUPPLEMENTARY NOTES Preprint--submitted to Surface Science		
19. KEY WORDS (Continue on reverse side if necessary and identify by block number) Thermal Desorption		
20. ABSTRACT (Continue on reverse side if necessary and identify by block number) Thermal Desorption of Xe from the (110) plane of tungsten can be followed layer by layer for 3 monolayers. In each case desorption is zero order until coverage is 0.3, when a sharp switch to first order occurs. The presence of even small amounts of oxygen kills the zero order regime in the first layer. Possible explanations for this behavior are given. The activation energies of desorption are shown to less than the corresponding enthalpies in each case, and the meaning of this result is discussed.		

DD FORM 1 JAN 73 1473

EDITION OF 1 NOV 65 IS OBSOLETE  
S/N 0102-014-6601

Unclassified

SECURITY CLASSIFICATION OF THIS PAGE (When Data Entered)

8 1 6 15 002

THERMAL DESORPTION OF Xe FROM THE W(110) PLANE

X

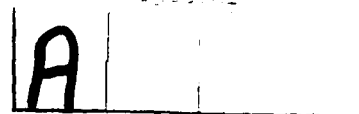
R. Opila and R. Gomer

The Department of Chemistry and The James Franck Institute

The University of Chicago, Chicago, Illinois 60637

ANALYSIS  
Spectra

ABSTRACT



The thermal desorption of Xe from the (110) plane of W was investigated.

Desorption could be followed layer by layer for 3 adsorbed layers, each containing equal amounts of Xe. In each case desorption rates were nearly coverage independent (i.e. of zero order) until  $\theta = 0.25\text{--}0.3$ , (in the layer under study) at which point a sharp transition to first order desorption occurred. If only 1 monolayer of Xe was adsorbed small amounts of preadsorbed oxygen led to first order desorption over the entire coverage regime. Possible mechanisms for the zero order regime in terms of desorption from the edges of islands with constant total island perimeter, or via a more complicated mechanism are given. The activation energies of desorption are shown to be less than the enthalpies of desorption for all layers and the meaning of this result is discussed. Results for Xe adsorbed on O/W layers preheated to 90K and 900K are also presented.

INTRODUCTION

The desorption of inert gases from metal surfaces would seem to present a particularly simple example of desorption kinetics since the complications of dissociation on adsorption and recombination on desorption are absent. One example in the literature, the study of Erikson and Yates[1] on the desorption of Xe from the W(111) surface in fact seems to bear this out. Desorption was found to be first order with an activation energy of 9.3 Kcal/mole and a fre-

quency factor of  $\sim 10^{15} \text{ sec}^{-1}$ . Some indication of possible complexities in such systems came from the work of Wang and Gomer[2] who found remarkably large effects of coadsorbed oxygen on the work functions and desorption temperatures of Xe on W(110) and W(100). The present work reveals some additional surprises. In brief, it was found that desorption could be followed layer by layer for at least 3 ad-layers and that in each case desorption was initially of zero order, until roughly 0.75 of a given layer had been desorbed; at this coverage desorption became first order. For the first adsorbed layer a very small amount of preadsorbed oxygen sufficed to make desorption first order over the entire Xe coverage range. Perhaps even more surprising, it was found that in each case the activation energy of desorption was substantially less than the corresponding enthalpy.

#### EXPERIMENTAL

The apparatus used in these experiments has been described in detail previously [3]. Use of the cryoshielded effusion source made it possible to deposit Xe only on the front surface of the crystal, which was kept at  $\sim 27\text{K}$  during deposition. Most of the experiments were performed with the cryoshield slit so wide that the entire length of the crystal received a gas deposit. In order to avoid possible effects from the ends of the current or potential leads and to improve temperature uniformity, some experiments were also carried out with a reduced slit length, so that only the central 10 mm portion of the crystal, located between the potential leads, received a Xe deposit. It was possible to verify this adsorbate geometry, and in fact, to ascertain the correct positioning of the crystal in front of the source by means of Auger measurements in which the Xe signal was measured as function of the lateral displacement of the crystal relative to the Auger beam. Temperature programmed and isothermal

desorption sequences utilized a new temperature controller, recently described in some detail [4]. For most experiments desorption rates were measured directly with a UTI C-100 quadrupole mass spectrometer. For coverages of  $< 1$  monolayer the amount of Xe remaining on the surface was also determined from the intensity of the Xe MNN Auger transition. In these measurements heating sequences were interrupted to make Auger measurements to avoid the effects of magnetic fields from the dc heating current and ESD from the Auger beam, which occurred only at  $T > 70K$ .

Relative coverages were most easily determined from the thermal desorption spectra themselves, but could also be found from the dosing times, once that for monolayer coverage had been established. Oxygen coverages were determined from Auger intensities, relative to the O/W = 0.5 layer.

The temperature calibration of the crystal has been described previously[4].

#### RESULTS

Fig. 1 shows temperature programmed spectra for coverages  $\theta$ ,  $2 < \theta \leq 3$ , for the whole front surface of the crystal. 3 distinct peaks are clearly discernible, with those corresponding to 1 and 2 layers remaining unchanged, while that corresponding to the 3rd layer diminishes in size with decreasing  $\theta_3$ . Moreover, the leading edge of the third layer peak remains unchanged, indicating zero order desorption. This will be shown in greater detail by the isothermal results. Fig. 2 shows desorption spectra for  $1 < \theta \leq 2$ . Here the spectrum of the first layer remains unchanged, while that of the second decreases in size as  $\theta_2$  decreases. The leading edge of the second layer peak again remains unchanged as  $\theta_2$  decreases. In Fig. 1 the time scale is drawn linearly so that the areas under the second plus third layer peaks (for a full 3rd layer) are twice that of the first layer. In Fig. 2 the curves have been redrawn to linear temperature scale so that the area under the first layer peak appears too small.

Fig. 3 shows desorption spectra for  $\theta < 1$ . Again the leading edge of the peak is unchanged, except for very low initial coverages. Essentially identical results were obtained by dosing only the central portion of the crystal.

The details of the desorption kinetics are brought out more clearly by isothermal sequences. Figs. 4-6 show such data for desorption in the first, second and third layers, respectively. In each case the desorption rate is almost coverage independent for  $\theta > 0.7$  (within a given layer). There is a sharp break at this critical  $\theta$ , and for lower coverages the rate decreases rapidly with decreasing  $\theta$ . Figs. 7-9 show that plots of  $i_{MS}$  vs. time (where  $i_{MS}$ , the mass spectrometer current, is proportional to desorption rate) are then linear, indicating first order desorption in this regime. These results were obtained for both Xe deposit geometries. Evidence for the existence of at least 3 uniform ad-layers also comes from the fact that the W Auger signal intensity decreases monotonically with Xe coverage. If there were some Xe crystallite formation, instead of adsorption layer by layer, this would not be the case.

Even small amounts of preadsorbed oxygen lead to a disappearance of the quasi-zero order regime in the first layer. Fig. 10 shows isothermal desorption for  $O/W = 0.5$  (adsorbed at 27 K and heated for 30 sec to 90 K before recooling and Xe adsorption) for a saturated Xe monolayer. Desorption is now first order over the entire coverage range. Disappearance of the quasi-zero order regime occurs when  $O/W > 0.04$ .

The effect of small amounts of oxygen on the rate suggests that the zero order regime is not the result of an experimental artifact, connected for instance with pumping speed effects or with temperature anisotropies over the crystal. The first of these points could be checked by suddenly turning off

the temperature controller. The mass spectrometer signal returned to zero almost instantaneously. The second point was checked by dosing the central portion of the crystal to monolayer coverage and then heating to 66 K for 90 sec, so that, according to curves like those of Fig. 4 the remaining coverage should have been 0.8. The crystal was then displaced parallel to its major dimension and the intensity of the Auger signal determined at each position. No difference could be discerned within experimental error, indicating that the Xe distribution remained uniform. It is most unlikely that diffusion could be rapid enough at 60-80 K to achieve a substantial redistribution of adsorbate. Consequently, the temperature must have been quite uniform over the central 10 mm portion of the crystal.

Experiments were also carried out for  $\theta < 1$  in which the coverage remaining on the surface was determined from the peak to peak separation of the second derivative of the Auger MNN transition. Results obtained in this way are shown in Fig. 11 and indicate that the coverage decreases linearly with time (as it should) in the quasi-zero order desorption regime.

In order to obtain the zero-order rate constants  $k_0$  we need to know  $(c/A)$  in the relation

$$ci_{MS} = - A \frac{d\theta}{dt} \equiv k_0 A \quad (1)$$

where  $i_{MS}$  is the mass spectrometer signal,  $c$  a proportionality constant,  $A$  the area of the crystal and  $\theta$  the coverage in atoms/cm<sup>2</sup>. It is known from the measurements of Wang and Gomer [2] that the maximum monolayer coverage  $\theta_0 = 6.6 \times 10^{14}$  at/cm<sup>2</sup>. Since the total area under curves like those of Fig. 3 corresponds to  $\theta_0$  we can find  $(c/A)$  from

$$c/A = \theta(t)/(i_{MS} t) \quad (2)$$

where  $\theta(t)$  is a coverage decrement, obtained from the relevant fraction of the

total area under the  $i_{MS}$  vs.  $t$  curve corresponding to a time  $t$ . Alternatively it is possible to determine the first order rate constant,  $k_1$ , from the relation,

$$(c/A) : MS = -d\theta'/dt' = k_1 \theta'_0 e^{-k_1 t'} \quad (3)$$

where  $\theta'_0$  is the coverage where first order desorption starts and  $t'$  the time measured from this point:

$$k_1 = -d(\ln i_{MS})/dt' \quad (4)$$

$k_1$  can then be used in Eq. 3, for instance at  $t' = 0$  to determine  $(c/A)$ . Both methods give the same result from which the absolute values of  $k_0$  can be found. Figs. 12-14 shows plots of  $\ln k_0$  vs.  $1/T$  for the initial zero order desorption rates in the first, second, and third layers. Straight lines are obtained and yield values of the corresponding activation energies which are listed in Table 1.

#### 1. Writing

$$k_0 = v_0 e^{-E/kT} \quad (5)$$

we can then combine these activation energies with the absolute values of  $k_0$  to obtain the corresponding  $v_0$  values, also listed in Table 1. The same values were obtained by plotting the logarithms of the times required for desorption to some constant coverage (still in the zero order regime) vs.  $1/T$ . Figs. 15-17 shows plots of  $\ln k_1$  vs.  $1/T$  for the first order desorption regimes in the first, second, and third layers respectively. The corresponding activation energies and frequency factors are listed in Table 1.

As already pointed out, preadsorbed oxygen in amounts  $O/W > 0.04$  led to first order desorption in the first layer. Fig. 18 shows a temperature programmed desorption spectrum, starting with 2.7 monolayers of Xe for surfaces precovered with  $O/W = 0.5$  preheated to 90 K and 900 K. For both conditions, the desorption peak of the first layer is shifted to increased temperatures. For  $O/W = 0.5$ , 900 K, there is also a long, low temperature

tail, which will be discussed presently. It is interesting that adsorbed oxygen also affects the second Xe layer, but not the third. Fig. 18 shows clearly that the second layer peak is shifted to lower temperature by the presence of oxygen, while the third layer peak is not affected. Oxygen precoverage does not remove the zero order regime for the second layer.

Activation energies and prefactors for various oxygen precoverages heated to 90 K were obtained for the first Xe layer. The results, (Figs. 19 and 20), show considerable scatter, but indicate a slight increase in E and a decrease in v with increasing coverage. Perhaps more significant are the values of  $k_1$  at a fixed temperature of 76.5 K vs. oxygen coverage, shown in Fig. 21. These indicate a systematic decrease of  $k_1$  in the range  $0.05 < O/W < 0.12$ , followed by a levelling off.

Isothermal desorption from surfaces covered with oxygen to the extent of  $O/W = 0.5$  preheated to 900 K reveal three distinct desorption regimes. Starting with a full Xe monolayer on the central portion of the crystal, there is desorption of 0.25 layers in the temperature range 62 - 75 K. The desorption of this fraction can be approximated by 2 first order regimes with activation energies of 2.8 and 2.7 Kcal/mol and pre-exponentials of  $5 \times 10^7$  and  $2 \times 10^8 \text{ sec}^{-1}$  respectively. When the entire face of the crystal was dosed, the results were  $E = 3.5$  and  $3.4 \text{ Kcal/mole}$  respectively and  $v = 2 \times 10^{10} \text{ sec}^{-1}$  for both. After desorption of this fraction, (for central dosing), another 0.2 layers desorb in the range 72-78 K, with  $E = 5.8 \text{ Kcal/mole}$  and  $v = 6 \times 10^{15} \text{ sec}^{-1}$ . Finally, the remainder, corresponding to 0.55 layers, desorbs in the range 78-86 K with  $E = 6.15 \text{ Kcal/mole}$  and  $v = 2 \times 10^{15} \text{ sec}^{-1}$ . When the entire front surface of the crystal was dosed, these last 2 states were not resolved and a single regime with  $E = 6.4 \text{ Kcal/mole}$  and  $v = 8 \times 10^{15} \text{ sec}^{-1}$  was seen for the terminal 0.55 monolayers.

This complex behavior is indicated qualitatively by the relevant desorption spectrum of Fig. 18. Fig. 22 shows plots of  $\ln k_1$  vs.  $1/T$  for the three regimes, including the decomposition of the lowest temperature regime into 2 exponentials.

The results for precoverage with oxygen at 90 and 900 K are in remarkably good agreement with the qualitative results obtained by Wang and Gomer [2] for similar conditions, although these authors could only obtain somewhat indirectly, crude "step desorption" spectra. In particular, they concluded that heating an oxygen layer to 900 K led to 3 distinct adsorption states for Xe, and that pre-heating to 90 K increased the desorption temperature of Xe.

It is interesting that the desorption data obtained for the first order regime, with only the center of the crystal covered with Xe, yield more finely resolved regimes probably because of the slightly more uniform temperature near the center of the crystal and the absence of surface heterogeneities like the ends of leads.

#### DISCUSSION

##### Zero-Order Desorption

The most striking feature of the present results is the occurrence of zero-order desorption, followed by a sharp transition to first order desorption. Zero-order desorption has also been seen in a number of other systems, e.g., Hg on W(100) [5], Ag on Ge (111) [6], Zn on GaAs [7], and Xe on graphite (1000) [8]. Several explanations to account for this behavior have been advanced, but none of these really explain our results satisfactorily.

We will presently show that the formation of close packed islands is probably involved, but not in a simple way. We first indicate why most island mechanisms cannot explain the observed behavior.

- 1) Desorption from the edge of islands, the number of islands  $N$  remaining

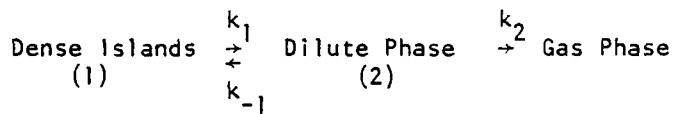
fixed. In this case desorption is of 1/2 order and can be shown to have the form

$$\frac{dg}{dt} = - \frac{dn}{dt} = 2 k_1 (\pi/\theta_1)^{1/2} N n^{1/2} \quad (6)$$

where  $n$  is the total number of atoms on the surface, and  $g$  the number of desorbed atoms.  $\theta_1$  is the (constant) density in atoms/cm<sup>2</sup> within each island.  $k_1$  is the desorption rate constant.

2) Desorption from the second layer, (relative to that from which desorption occurs); i.e. from the tops of islands,  $N = \text{constant}$ . If the second layer is populated from the edges of islands, the kinetics are as in (1). If the second layer is populated from within the island, kinetics are first order, as can be shown trivially.

3) Detachment into a dilute phase, desorption from the dilute phase,  $N = \text{constant}$ .



We have for this assumed mechanism

$$\frac{dn_2}{dt} = k_1 N 2\pi r \quad (7)$$

$$-\frac{dn_2}{dt} = k_{-1} N 2\pi r (n_2/A_2) + k_2 n_2 \quad (8)$$

where  $r$  is the mean island radius and  $A_2$  the area of the dilute phase. Assuming steady state for the total number of atoms in the dilute phase,  $n_2$

$$n_2 = \frac{k_1 N 2\pi r A_2}{k_{-1} N 2\pi r + k_2 A_2} \quad (9)$$

Since

$$r = \left( \frac{n_1}{\theta_1 \pi} \right)^{1/2} \quad (10)$$

where  $n_1$  is the number of atoms in an average island, and  $\theta$  the (constant) density within each island, we obtain

$$\frac{dg}{dt} = - \frac{dn}{dt} = k_2 \frac{\frac{k_1 N 2(\pi/\theta_1)^{1/2} n_1^{1/2}}{k_{-1} N 2(\pi/\theta_1)^{1/2} n_1^{1/2} + k_2 (A-A_1)}}{(A-A_1)} \quad (11)$$

where we have replaced  $A_2$  by  $A-A_1$ ,  $A_1$  being the area occupied by islands. If

$$k_{-1} N_2 (\tau/\theta_1)^{1/2} n_1^{1/2} \ll k_2 (A-A_1) \quad (12)$$

we obtain Eq. (6), although in principle  $k_1$  now refers to detachment only.

If inequality (12) is reversed we find

$$-\frac{dn}{dt} = K k_2 (A-A_1) \quad (13)$$

where

$$K \equiv \frac{k_1}{k_{-1}} = \frac{n_2}{A_2} = \theta_2 \quad (14)$$

with the second equality following from Eq. (9) with the reversed inequality

(12). Under these conditions  $\theta_2 = \text{constant}$ . Since

$$-dn = -\theta_1 dA_1 - \theta_2 dA_2 \quad (15)$$

and since

$$dA_1 = -dA_2 \quad (16)$$

we easily find from Eq. (13) that

$$-\frac{dn}{dt} = \frac{dg}{dt} = K k_2 A_2(0) \exp\left(\frac{Kk_2}{\theta_1 - \theta_2} t\right) \quad (17)$$

i.e. exponentially increasing desorption, assuming a small but finite area  $A_2(0)$  available to the dilute phase at time  $t = 0$ . When only the dilute phase remains desorption would become first order, i.e.  $dg/dt$  would then decrease exponentially. Thus, none of the cases so far considered lead to anything resembling zero order kinetics. While it is true that Eq. 13 corresponds to constant, equilibrium concentration in the dilute phase, the area of the dilute phase increases as desorption proceeds thus leading to exponentially increasing desorption as just shown.

4) Attractive interactions between ad-atoms without explicit island formation.

In this case the qualitative behavior is in the right direction. As the adsorbate concentration decreases, the ad-ad interactions play a decreasing role thereby decreasing  $E_{des}$  and compensating for the decrease in rate which would otherwise occur. Figs. 23-24 show the results of Monte-Carlo calculations for various assumed Xe-Xe interaction parameters. If the interaction is too weak, quasi-first order desorption results. If it is too strong, an initial increase in rate followed by a decrease occurs. Such peaking was also found by Jones and Perry[9]. In no instance was it possible for us to obtain behavior in which the change from quasi-zero order to first order was either abrupt or occurred at the correct coverage. The results were not improved by including diffusion either with the same or with different interaction parameters as for desorption. Some details of these calculations are given in Appendix I.

We come finally to two mechanisms involving islands which can explain the results. Desorption from the edges of islands, either directly into the gas phase, or first into a dilute phase with high probability of subsequent desorption, leads to zero order kinetics if the total periphery of all islands remains constant. This is, in fact, not unreasonable. At a critical coverage, depending slightly on temperature, islands break up completely and desorption then proceeds via first order kinetics. This transition can be quite sharp accounting for the sharp break in the curves of Figs. 4-6. In the zero order regime we have for this mechanism

$$\frac{dg}{dt} = k_0 A = 2\pi r N k_1 = 2\pi r (N/A) A k_1 \quad (18)$$

where all symbols have the same meaning as in Equations 6-17. Thus,

$$k_0 = 2\pi r (N/A) k_1$$

As here defined  $k_1$  is the rate of evaporation per unit line length. In terms of the effective frequency of atomic vibration,  $v_1$ , and the activation energy,

E per atom, we can write

$$k_1 = (v_1 e^{-E/kT})/d_{Xe} \quad (19)$$

where  $d_{Xe} \approx 3 \times 10^{-8}$  cm represents the perimeter length per Xe atom. Thus, we can write

$$v_o = 2\pi r (N/A) (v_1/d_{Xe}) \quad (20)$$

We assume, to keep the kinetics zero order, that  $2\pi r (N/A) = \text{constant}$ .

If we assume that  $v_1 = 10^{12}$  sec<sup>-1</sup> we see from Eq. 20 and from the experimental value  $v_o = 1 \times 10^{25}$  for the first layer that  $2\pi r (N/A) = 3 \times 10^5$  cm<sup>-1</sup>. Since

$$(N/A)\pi r^2 \ll 1 \quad (21)$$

we find that  $r_{\max} = 6 \times 10^{-6}$  cm. Thus, the assumption of desorption from island edges with the total periphery constant is consistent with the experimental value of  $v_o$  and a reasonable choice for  $v_1$  if the maximum average island radius is  $\sim 10^{-5}$  cm. For the second and third layers, even larger values of  $r_{\max}$  are allowed.

There is a second possible mechanism involving islands. It is based on the following assumptions:

- 1) Desorption occurs only when a Xe atom has become detached from an island, i.e., is in the dilute phase. 2) At the desorption temperature, Xe atoms move so rapidly, and their concentration in the dilute phase is so small that their mean free path is limited by collisions with islands to which they become reattached upon collision. The decrease, if any, in detachment rate because of decreasing island perimeter is then exactly balanced by an increase in the mean time between atom-island collisions since the former is proportional to island radius and the latter inversely proportional to this quantity. The time  $t_c$  between collisions, i.e., the mean free time of Xe atom in the dilute phase is:

$$t_c = [\bar{v} (d + d_{Xe}) (N/A)]^{-1} \quad (22)$$

where  $d$  is the mean island diameter and  $d_{Xe} = 3 \times 10^{-8}$  cm that of a Xe atom.

$\bar{v}$  is the mean thermal velocity of Xe atoms in the dilute phase. The desorption rate is then

$$\frac{dg}{dt} = \frac{t_c}{\tau} \pi d \cdot N k_1 = \frac{\pi k_1 k_2 A}{\bar{v}} \left( \frac{d}{d + d_{Xe}} \right) \quad (23)$$

where  $\tau \equiv 1/k_2$  is the lifetime of a Xe atom in the dilute phase and  $k_1$  the detachment rate constant from the island edge into the dilute phase. If  $d_{Xe} \ll d$  desorption is zero order without any assumptions about the constancy of the island perimeter or changes in the number of islands. A sharp transition to first order will occur if islands disappear while  $d$  is still somewhat larger than  $d_{Xe}$ . For this mechanism

$$k_o = k_1 k_2 \pi / \bar{v} \quad (24)$$

and the experimental activation energy is the sum of the detachment and evaporation activation energies. Consequently, we may write

$$v_o = v_1 v_2 \pi / (3 \times 10^{-8} \bar{v}) \quad (25)$$

Assuming  $\bar{v} = (kT/2m)^{1/2} = 4.7 \times 10^3$  cm/sec at 70 K and taking  $v_2$  from the first order regime to be  $4 \times 10^{12} \text{ sec}^{-1}$ , we find  $v_1 = 1 \times 10^8 \text{ sec}^{-1}$  for this mechanism. This is rather small, but not impossible.

It is interesting that the activation energies for zero and first order kinetics are almost identical within experimental error, and that the presence of preadsorbed O also affects E only very slightly. This indicates that very small energy differences determine which regime will be observed, and also explains why zero order desorption can be observed, even at full coverage, where presumably the island perimeters, (or the distance between islands), are zero not counting the external edge of the layer. Adsorbed oxygen presumably inhibits island formation, possibly because the O-Xe interaction predominates over the Xe-Xe interaction. Although the Monte-Carlo calculations mentioned

earlier do not give a quantitative description of the observed desorption behavior, they come rather close. It is probably significant that the best fit is obtained for Xe-Xe interactions of 45 cal/mole, a very small energy relative to the (4000 cal/mole) activation energy of desorption in the first layer.

#### Activation Energies of Desorption

The enthalpy of sublimation of bulk Xe is 3.7 Kcal/mole. Thus, even in the first layer, the activation energy is only very slightly greater than the Xe sublimation enthalpy. In the second and third layers, the activation energies of 3.2 and 2.9 Kcal are substantially less. Since the entropies of bulk Xe and adsorbed Xe layers must be comparable, it follows that the enthalpies of adsorption must exceed that of bulk Xe or the adlayers would be unstable with respect to the latter. There is absolutely no evidence of such instability up to at least three adsorbed layers. Consequently, we can conclude that the activation energies in the second and third layers are definitely less than the corresponding enthalpies. Even in the first layer this is almost certainly the case. Previous work[10], suggests that the enthalpy of adsorption in the first layer is closer to 10 Kcal/mole than to 4 Kcal/mole.

Thus, we have here a quite clearcut case of activation energies less than corresponding enthalpies. A similar situation was encountered by us for weakly adsorbed molecular oxygen both,  $\alpha$ -O<sub>2</sub> and physisorbed O<sub>2</sub>, which exist on a W(110) surface precovered with atomic O[4]. Such behavior has been predicted theoretically by Freed and coworkers [11]. Their explanation, at least qualitatively, is the following. The potential energy curve corresponding to the motion of the adsorbate normal to the surface deviates from that of a harmonic oscillator as the surface-adsorbate distance increases. In the anharmonic region the density of states increases rapidly with increasing energy and if this degree of freedom is excited to a certain critical energy

which may lie quite appreciably below that corresponding to desorption, the probability that the adsorbate will gain enough energy from multi-phonon processes to desorb is much greater than the probability that it will lose energy and return to the ground state by emitting one phonon at a time. Thus, the activation energy measured in a kinetic experiment corresponds to this critical energy rather than to the enthalpy of desorption. The extreme case of the situation just described can be represented as a two step mechanism for desorption: step 1 takes the system to the critical energy, and step 2 corresponds to desorption from this point. If step 1 is much slower than step 2, the overall rate is governed by its rate.

This can be formalized by the requirement that

$$\frac{v_1 e^{-E_1/kT}}{v_2 e^{-E_2/kT}} \ll 1 \quad (26)$$

or, since  $E_1 + E_2 = H$ , where  $H$  is the enthalpy of desorption, that

$$\frac{v_1}{v_2} \ll e^{(2E_1 - H)/kT} \quad (27)$$

#### Effect of Oxygen on Xe Desorption

Preadsorbed oxygen heated to 90 K appears to have only a small effect on the activation energy of Xe desorption. In view of the preceding discussion, it is not possible to equate this with an equally small effect on the enthalpy, but this seems probable. Discussions of why adsorbed O could affect the enthalpy of Xe adsorption have been given previously[2] and we have little to add.

The situation for 0 layers heated to 900 K is more intriguing. Approximately 0.45 of the Xe layer now desorbs with a smaller activation energy than on clean W, while ~0.55 desorbs with a higher one. For this fraction, the high value of  $v$  suggests that the activation energy is now fairly close to the enthalpy in

view of Eqs. (26) and (27). While no real conclusions about the effect on the enthalpy can be drawn, it appears that heating to 900 K leads to surface reconstruction which permits a part of the adsorbate to be in such contact with W atoms as to increase its binding energy while forcing a smaller fraction of Xe to be adsorbed in a way which actually decreases its binding energy. It is planned to investigate these points by means of UPS and XPS.

#### CONCLUSION

The results discussed here indicate that the adsorption of Xe on W(110) represents a very complicated system. The principal findings are the occurrence of zero order desorption in each adsorbed layer and clear evidence for activation energies less than the corresponding enthalpies. The latter finding indicates that one must be very cautious about equating activation energies with enthalpies of desorption, particularly for weak adsorption.

#### ACKNOWLEDGEMENT

This work was supported in part by ONR Contract N00014-77-C-0018. We have also benefitted from the Materials Research Laboratory of the National Science Foundation at The University of Chicago.

Appendix: Monte-Carlo Simulations of Desorption for Interacting Ad-particles

A Monte-Carlo simulation of desorption was carried out as follows: A square lattice was assumed with periodic boundary conditions. Pairwise nearest neighbor interactions  $J$  were assumed. Full coverage at the start of each run was chosen. In each complete computer pass each site was interrogated in random sequence once and only once. The desorption probability for each site in one such interrogation, (i.e., per computer step), was chosen to be

$$W = \tau_{\text{des}}^{-1} \exp(-nJ/kT) \quad \text{for an occupied site} \quad (\text{A1})$$

$$W = 0 \quad \text{for an empty site}$$

Attractive nearest neighbor interactions correspond to negative values of  $J$ .  $\tau_{\text{des}}$  corresponds to the mean lifetime with respect to desorption in the absence of interactions, i.e. at zero coverage:

$$\tau_{\text{des}} = v^{-1} \exp(E_{\text{des}}^0/kT) \quad (\text{in seconds}) \quad (\text{A2})$$

where  $v$  is a frequency factor and  $E_{\text{des}}^0$  the zero coverage activation energy of desorption. Since  $\tau_{\text{des}}$  is expressed in real time, this fixes the scale of computer time as 1 second per step. This assignment is adequate for  $\tau \gg 1$  second, as was the case here. (In any case, a constant factor converting  $\tau$  from real to an arbitrary time scale could have been used if this condition were not met.) The probability of desorption according to Eq. A1 was then determined in a standard manner by assigning the appropriate weight to  $W$  in the interval 0-1 and picking a random number in this interval by means of a DEC pseudo-random number generator. The results of many runs from full coverage to zero coverage for a  $20 \times 20$  lattice were averaged to obtain the data shown in Fig. 23 which also shows the results of a real experiment. The Monte-Carlo results for  $J = -0.04$  Kcal/mole come closest to simulating the real experiment, but lack the sharp transitions from zero to first order.

Additional Monte-Carlo experiments were carried out to include the effect of diffusion. In principle, this can be done by sampling each site as before and dividing the number interval 0 - 1 into 3 segments corresponding to the probability of diffusion, desorption, or of no event. The probability of desorption is then given by Eq. A1, that of diffusion is given by

$$\begin{aligned} w_{\text{diff}} &= \tau_{\text{dif}}^{-1} \exp(-n \beta_{\text{dif}}/kT) \text{ if the site is occupied} \\ &= 0 \quad \text{if the site is empty} \end{aligned} \quad (\text{A3})$$

If the random number generator signals diffusion, a nearest neighbor site is then picked at random and if this site is empty, diffusion to it is carried out. If the site to which diffusion is proposed is filled, no event occurs. The difficulty with this approach is that the value of  $\tau_{\text{dif}}$  is so much less than that of  $\tau_{\text{des}}$  that each unit step can no longer be chosen as 1 second. If the values of Chen and Gomer[12] for Xe diffusion are chosen  $v_{\text{dif}} = 10^7 \text{ sec}^{-1}$  (assuming  $D_0 = 10^{-8} \text{ cm}^2 \text{ sec}^{-1}$ ) and  $E_{\text{dif}} \approx 1 \text{ Kcal/mole}$ ,  $\tau_{\text{dif}} = 1 \times 10^{-4} \text{ sec}$ . Experiments with an unrealistically small value of  $v_{\text{dif}} = 6.25 \times 10^2 \text{ sec}^{-1}$  and  $E_{\text{dif}} = 1 \text{ Kcal/mole}$  (giving  $D_0 = 5 \times 10^{-13} \text{ cm}^2 \text{ sec}^{-1}$ , and  $\tau_{\text{dif}} = 2$ ) were in fact carried out, and led to very little change from the previous results. Note that here  $\tau_{\text{dif}}/\tau_{\text{des}} = 0.1$ , so that quasi-equilibration occurs between desorption events.

A more realistic approach, given the disparity between  $\tau_{\text{des}}$  and  $\tau_{\text{dif}}$ , consists of making one desorption step as before, allowing the sample to equilibrate by means of standard Monte-Carlo procedure, (not counting in any way the time for this equilibration), and then proceeding to the next desorption step, etc. The results obtained in this way were not significantly different from the previous ones.

We would like to acknowledge many helpful discussions with Stanley Brooks and Jayanth Banaver about the Monte Carlo calculations.

TABLE 1

Summary of Desorption Results

Zero Order Regime			First Order Regime		
	$v_0$ (atoms sec $^{-1}$ cm $^{-2}$ )	E (Kcal/mole)		$v_1$ (sec $^{-1}$ )	E (Kcal/mole)
First Layer	$3 \times 10^{25}$ ( $10^{25}$ )	4.0 (3.9)		$1 \times 10^{12}$ ( $4 \times 10^{10}$ )	4.3 (3.9)
	$5 \times 10^{26}$ ( $2 \times 10^{26}$ )	3.3 (3.2)		$6 \times 10^{12}$ ( $3 \times 10^{10}$ )	3.3 (2.8)
3rd Layer					
	$(9 \times 10^{25})$	(2.9)		$(1.5 \times 10^{10})$	(2.5)

Values in parentheses refer to those obtained with entire front face of crystal covered with Xe.  
 Other numbers refer to Xe deposit only in central portion of the front face.

#### REFERENCES

- [1] J.T. Yates and N. Erikson, Surf. Sci. 44 (1974) 489.
- [2] C. Wang and R. Gomer, Surf. Sci. 91, (1980) 533.
- [3] Ch. Steinbrüchel and R. Gomer, Surf. Sci. 67 (1977) 21; R. Opila and R. Gomer, Surf. Sci. (in press).
- [4] H. Michel, R. Opila and R. Gomer, Surf. Sci. (in press).
- [5] R.G. Jones and D.L. Perry, Surf. Sci., 71 (1978) 59.
- [6] M. Bertucci, G. Le Lay, M. Manneville and R. Kern Surf. Sci. 85 (1979) 471.
- [7] J.R. Arthur, Surf. Sci. 38 (1973) 394.
- [8] M. Bienfait and J.A. Venables, Surf. Sci. 64 (1977) 425.
- [9] R.G. Jones and D.L. Perry, Surf. Sci. 82 (1979) 540.
- [10] T. Engel and R. Gomer, J. Chem. Phys. 52 (1970) 5572.
- [11] S. Efrima, K.F. Freed, C. Jedrzejek and H. Metiu, Chem. Phys. Lett. 74 (1980) 43.
- [12] J-R Chen and R. Gomer, Surf. Sci. 94 (1980) 456.

#### FIGURE CAPTIONS

- 1) Temperature programmed desorption for initial coverages in excess of 2 monolayers. Note the constant leading edge of the desorption peak of the third layer. The variation in peak height for the second layer peak is probably due to some overlap from the third layer peak. Entire front face of crystal covered with Xe.
- 2) Temperature programmed desorption for coverages in excess of 1 layer but less than 2 layers. Note the constant leading edge of the second layer peak. The apparent difference in area under the first and full second layer peaks is discussed in the text. Entire front face of crystal covered with Xe.
- 3) Temperature programmed desorption for  $\theta \leq 1$  monolayer. Note the constant leading edge of the peaks. Entire front face of crystal covered with Xe.
- 4) Isothermal desorption for initial coverage of 1 monolayer. Note the almost constant rate of desorption to  $\theta = 0.3$ . Initial fast decay is the result of temperature overshoot. Entire front face of crystal covered with Xe.
- 5) Isothermal desorption within the second layer. Entire front face of crystal covered with Xe.
- 6) Isothermal desorption within the third layer. Entire front face of crystal covered with Xe.
- 7) Semilogarithmic plot of mass spectrometer signal vs. time for first order regime for first Xe layer. Only the central portion of front face of crystal covered with Xe.
- 8) Semilogarithmic plot of mass spectrometer signal vs. time for first order regime in the second layer. Entire front face of crystal covered with Xe.
- 9) Semilogarithmic plot of mass spectrometer signal vs. time for first order regime in the third layer. Entire front face of crystal covered with Xe.
- 10) Mass spectrometer signal vs. time for isothermal desorption of Xe in the first layer for a surface precovered with oxygen and heated to 90 K before

## FIGURE CAPTIONS

- Xe adsorption. Entire front face of crystal covered with oxygen and Xe.
- 11) Ratio of Xe to W Auger intensities, determined from peak to peak amplitudes for the zero order regime in the first layer.
  - 12) Plot of  $\ln k_0$  for the first layer vs.  $1/T$ . All open points refer to runs with the entire front face of the crystal dosed, full points to a Xe deposit only on the central part of this face.
  - 13) Plot of  $\ln k_0$  for the second layer vs.  $1/T$ . All open points refer to runs with the entire front face of the crystal dosed, full points to a Xe deposit only on the central part of this face.
  - 14) Plot of  $\ln k_0$  for the third layer vs.  $1/T$ . All points were taken with the entire front face of the crystal dosed with Xe.
  - 15) Plot of  $\ln k_1$  vs.  $1/T$  for the first layer. Open points and solid line refer to entire front face of crystal covered with Xe, solid points and dashed line to Xe deposited only on the central portion of the face.
  - 16) Plot of  $\ln k_1$  vs.  $1/T$  for the second layer. Open point and solid line refer to entire front face of crystal covered with Xe, solid points and dashed line to Xe deposited only on the central portion of the face.
  - 17) Plot of  $\ln k_1$  vs.  $1/T$  for the third layer. Entire front face of crystal dosed with Xe.
  - 18) Temperature programmed desorption for 2.7 monolayers of Xe on surfaces pre-covered with oxygen and heated as indicated on the figure. Oxygen coverages in all cases  $O/W = 0.5$ . Note the effects on both the first and second layer peaks.
  - 19) Activation energy for first order regime in the first layer as function of oxygen coverage, expressed as  $O/W$ , for the oxygen layer heated to 90 K before Xe adsorption. Entire front face of crystal covered with oxygen and Xe.

#### FIGURE CAPTIONS

- 20) Prefactor of first order rate constant in the first layer as a function of oxygen coverage expressed as O/W, for the oxygen layer heated to 90 K before Xe adsorption. Entire front face of crystal covered with oxygen and Xe.
- 21)  $\ln k_1$  at 76.5 for first order desorption in the first layer as a function of oxygen coverage expressed as O/W, for the oxygen layer heated to 90 K before Xe adsorption. Entire front face of crystal covered with oxygen and Xe.
- 22)  $\ln k_1$  vs.  $1/T$  for desorption in the first layer from a surface precovered with oxygen,  $O/W = 0.5$  and heated to 900 K before Xe adsorption. Note 3 regimes. Entire front face of crystal covered with oxygen and Xe. Open points and solid lines refer to entire front face of crystal covered with Xe, solid points and dashed lines to Xe deposited only on the central portion of the face.
- 23) Monte-Carlo calculations of desorption rate  $\Delta n/\Delta t$  in atoms/second vs. real time for various assumed interaction energies  $J$ , shown on figure. The zero coverage desorption mean lifetime  $\tau_{des} = 23.1$  seconds. An experimental curve is also shown.
- 24) Monte-Carlo calculations of desorption for various assumed adsorbate-adsorbate interactions in desorption and different interactions in diffusion  $J_d$  shown on figure,  $\tau_{des} = 23.1$  sec,  $\tau_{dif} = 2.1$  sec.

Mass Spectrometer Signal (arb. units)

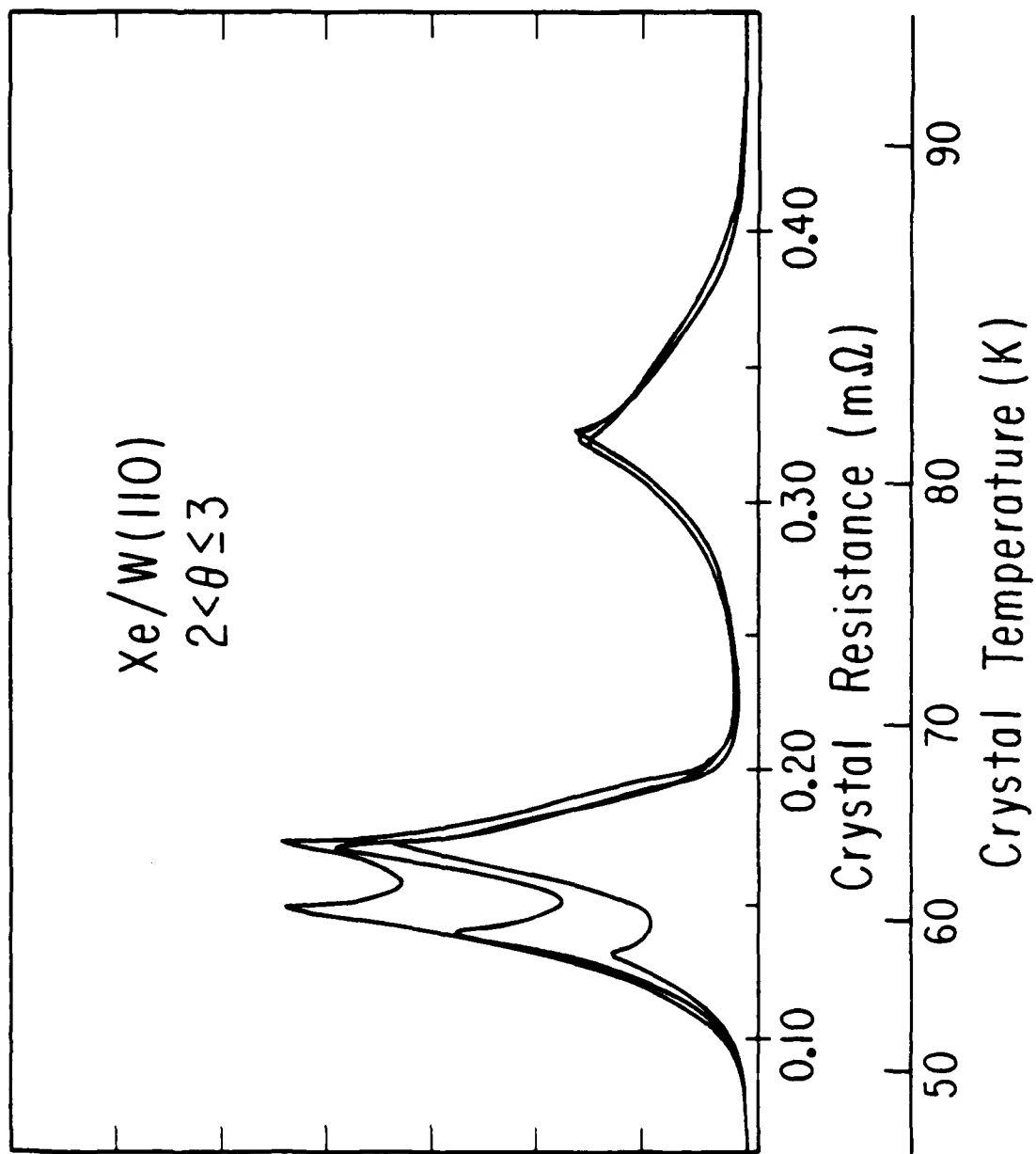


Fig. I

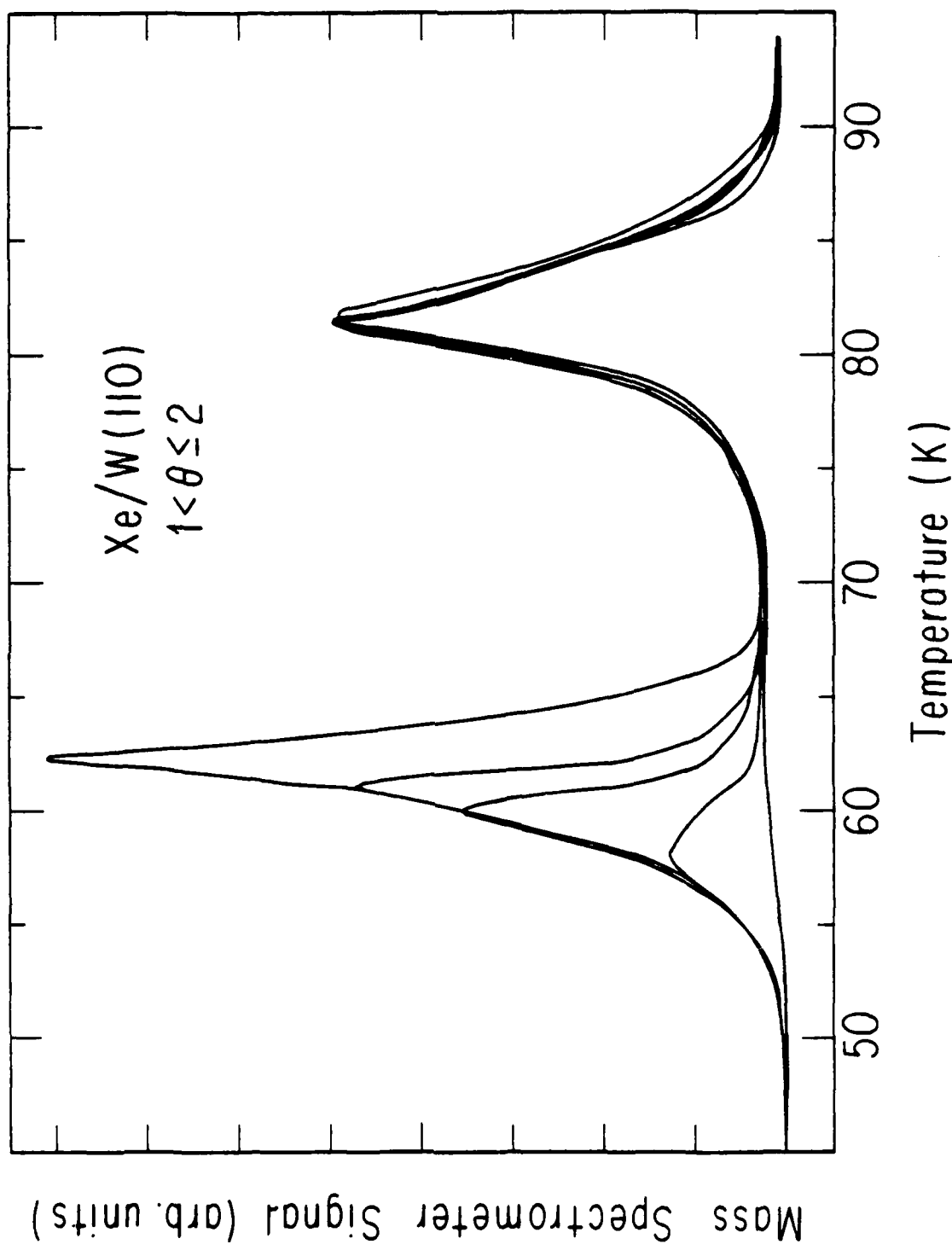


Fig.2

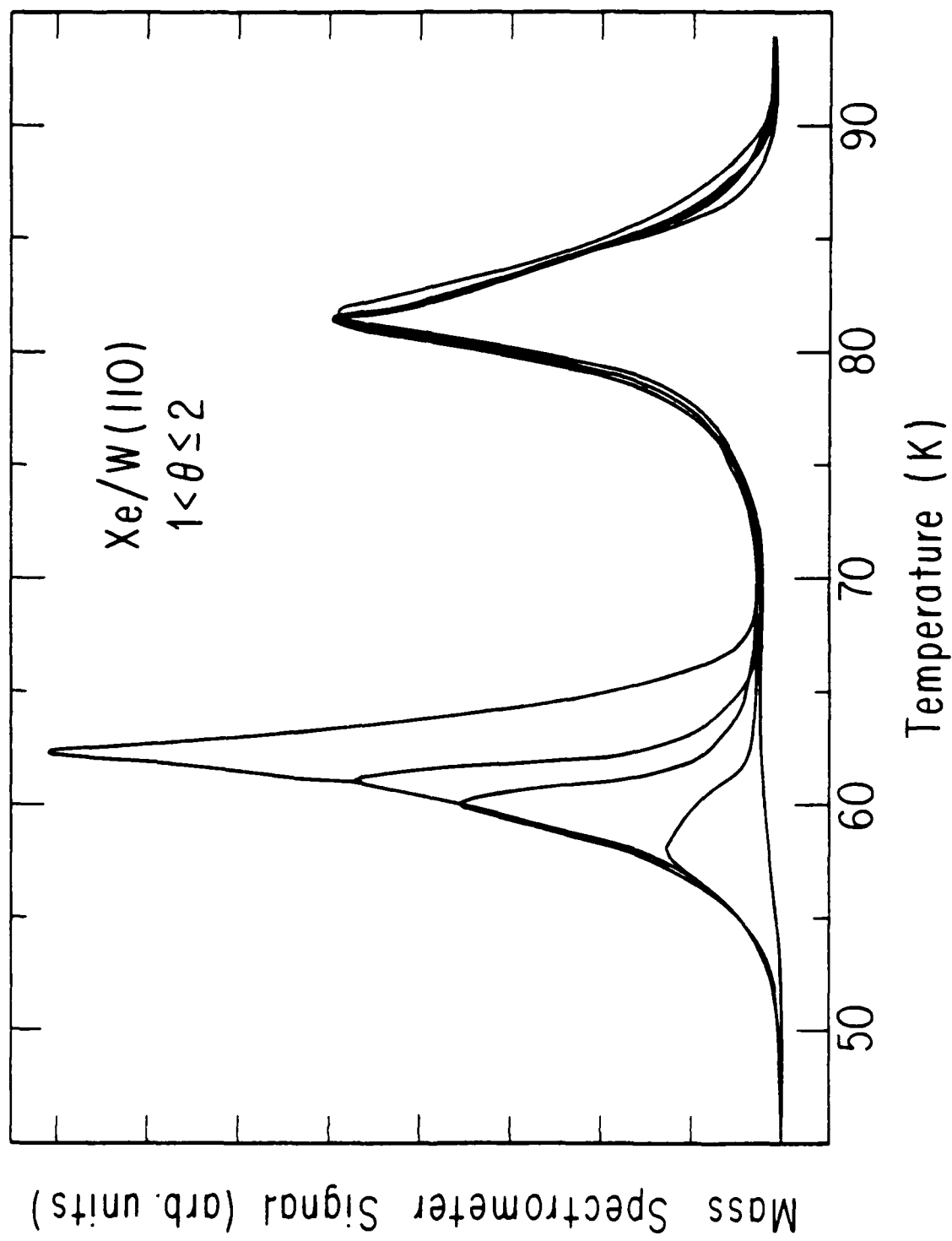


Fig. 2

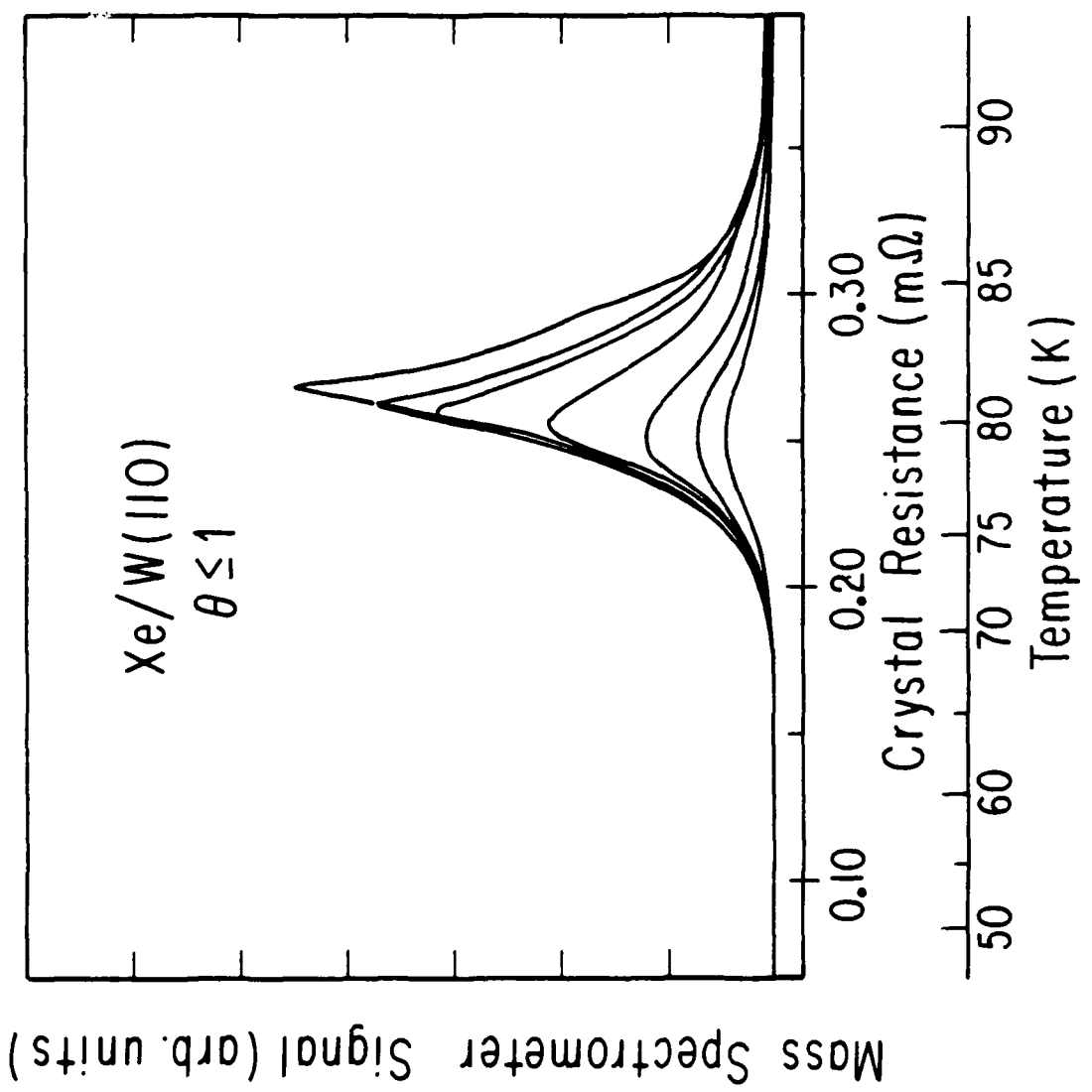


Fig.3

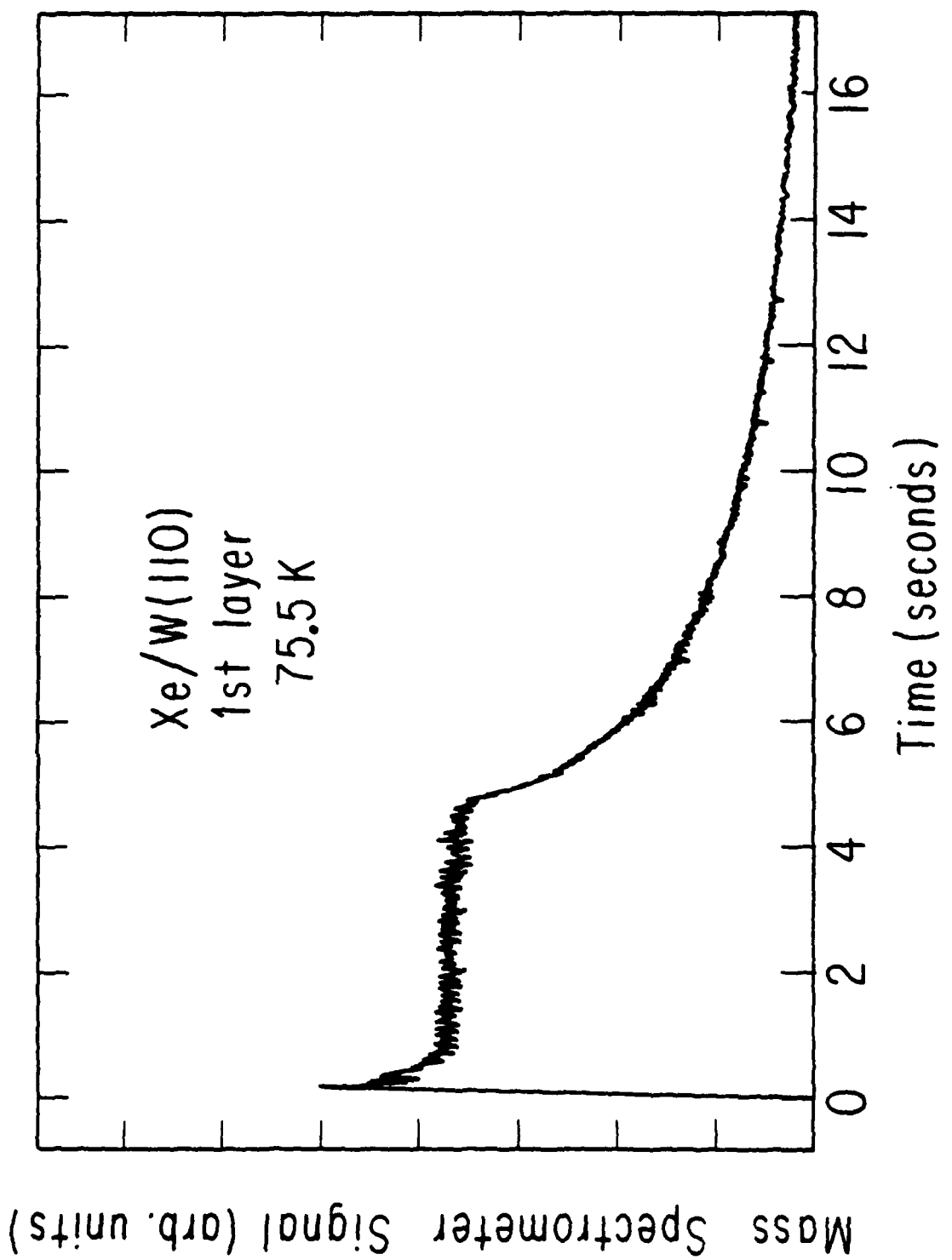


Fig.4

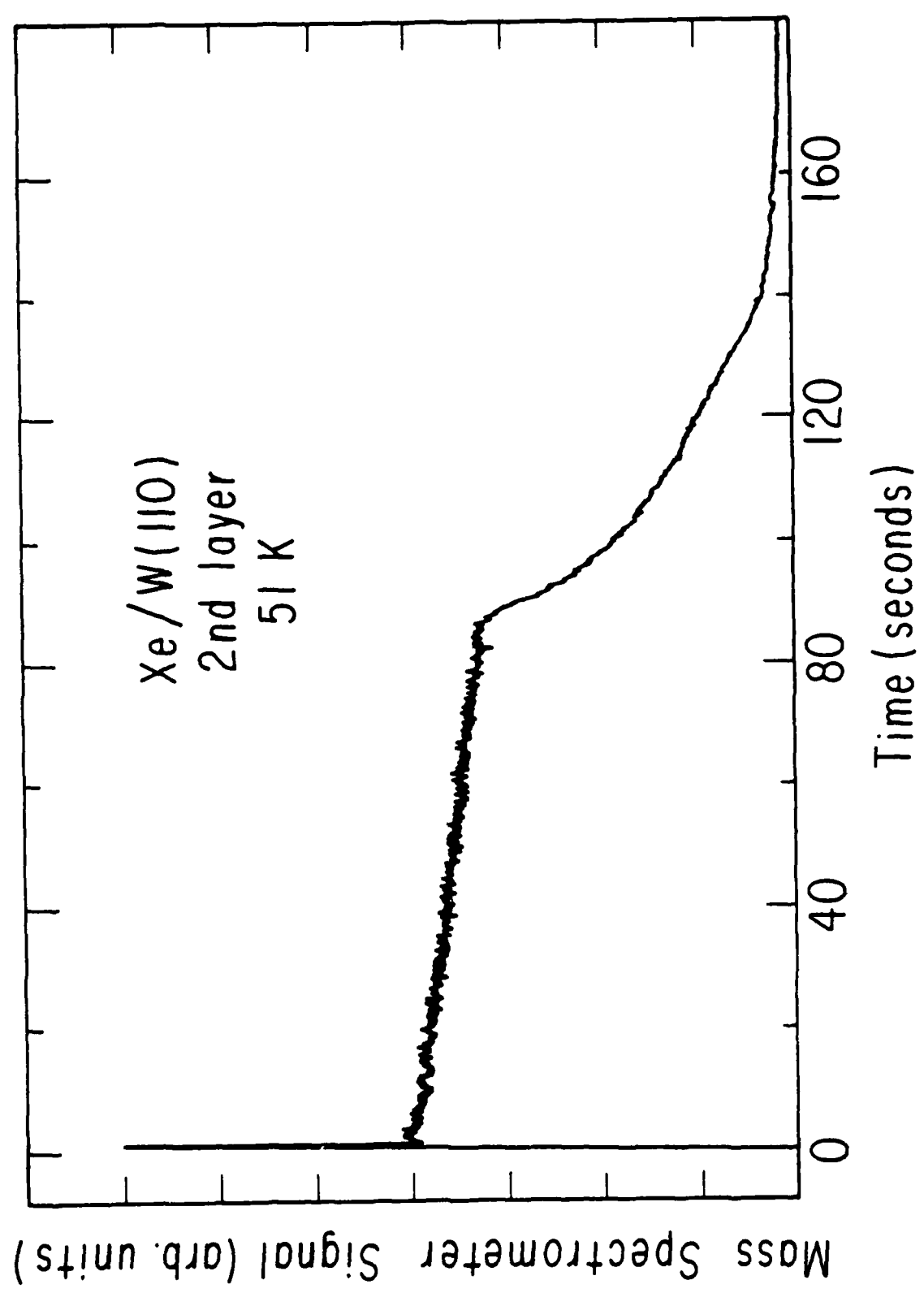


Fig.5

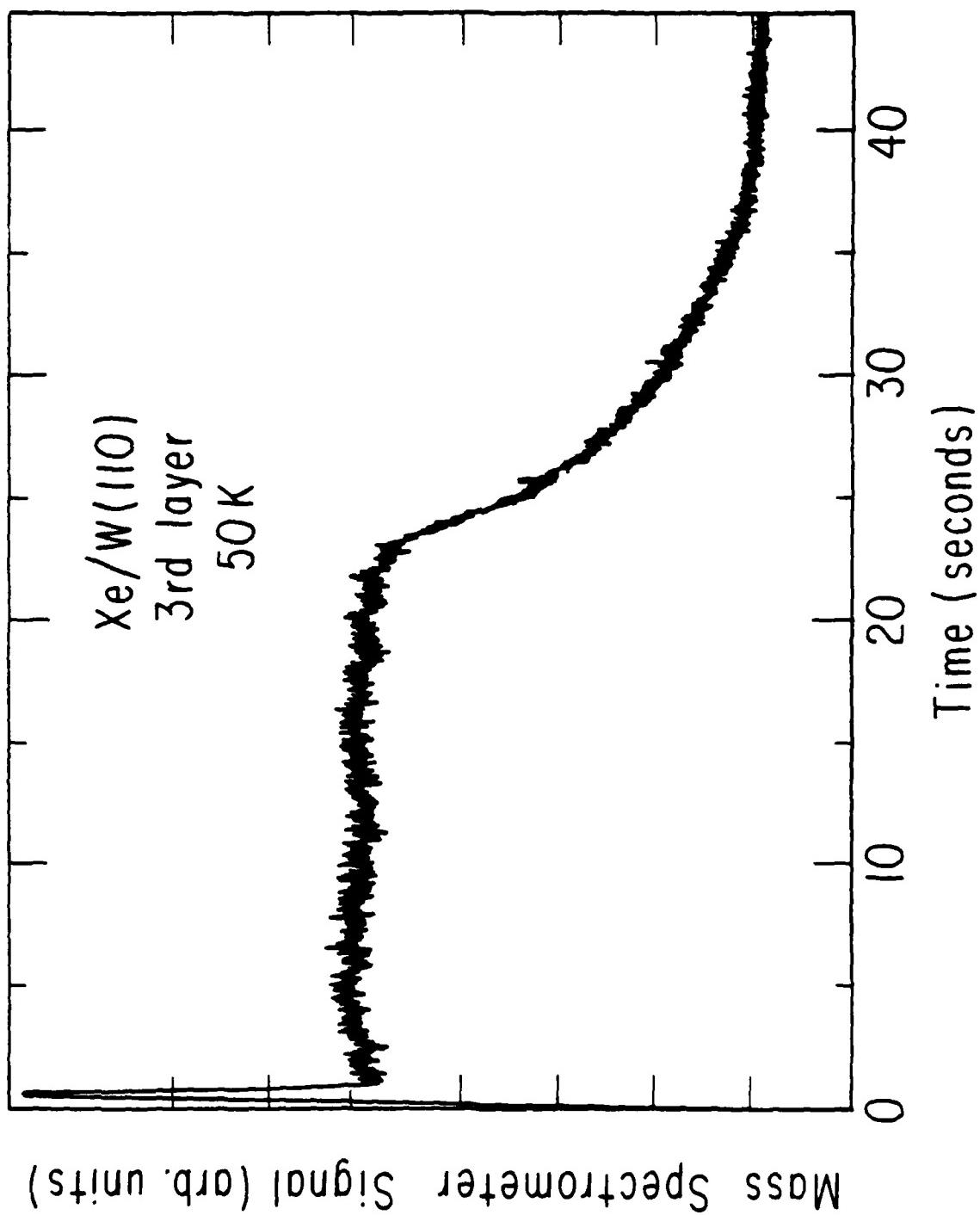


Fig.6

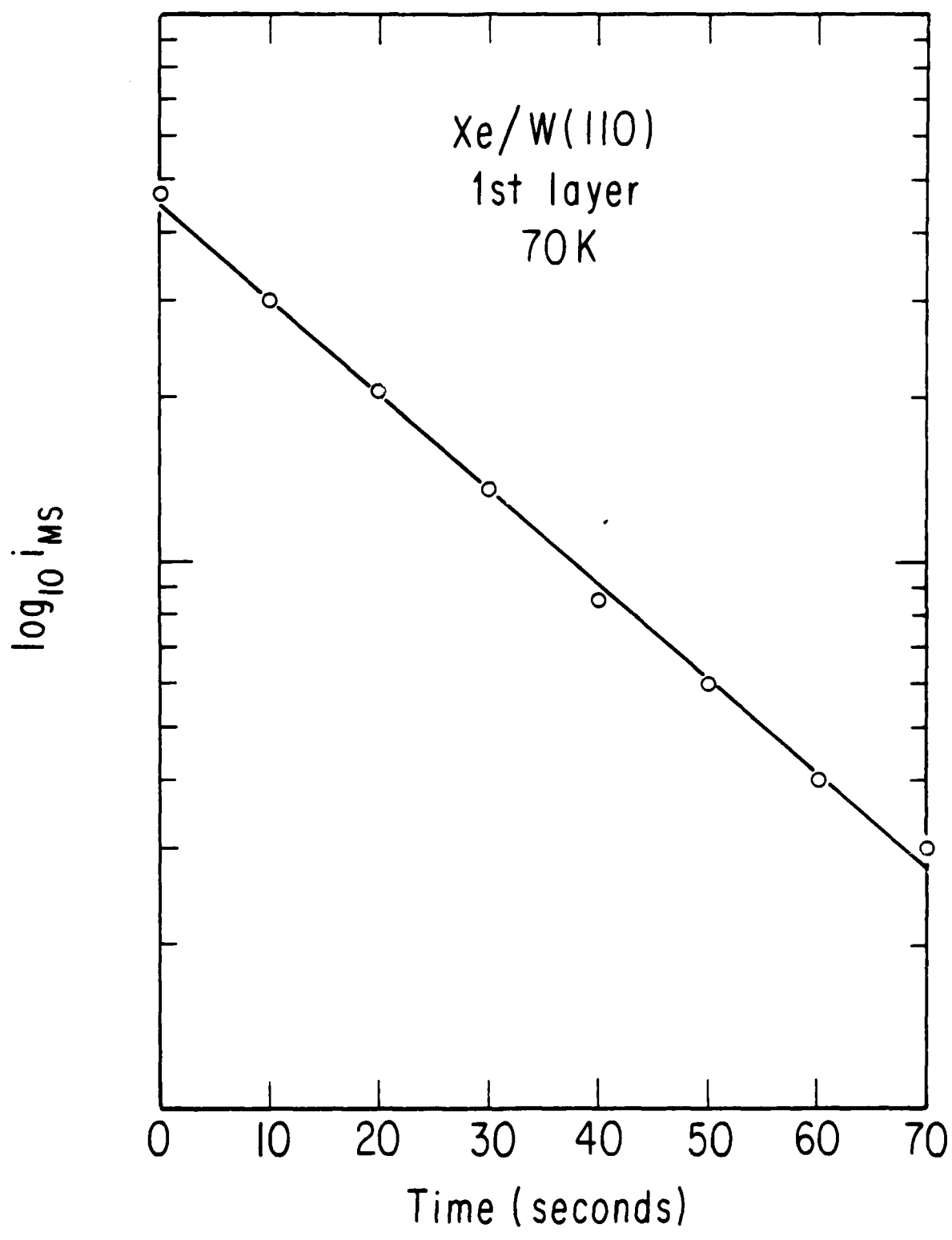


Fig.7

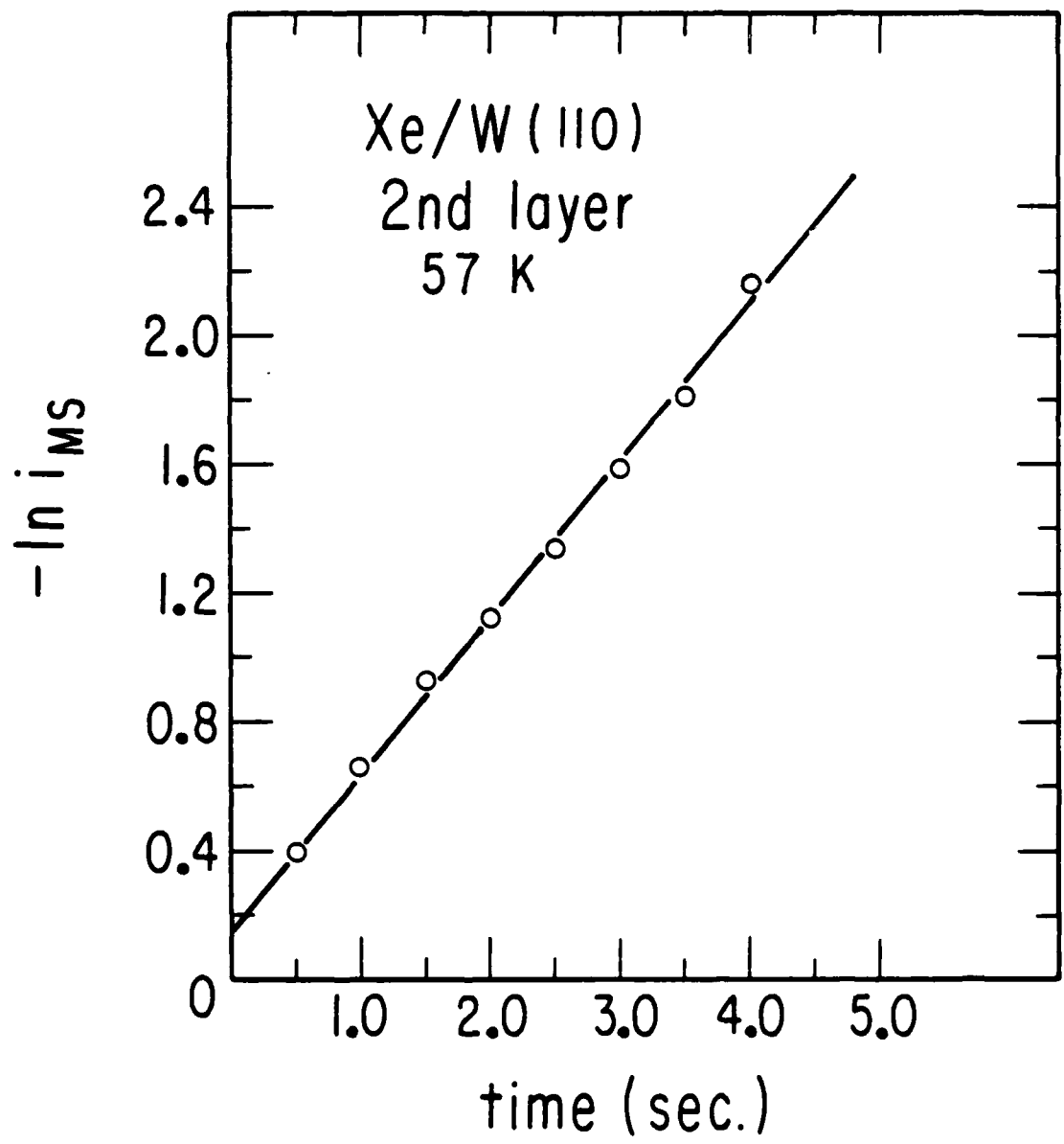


Fig. 8

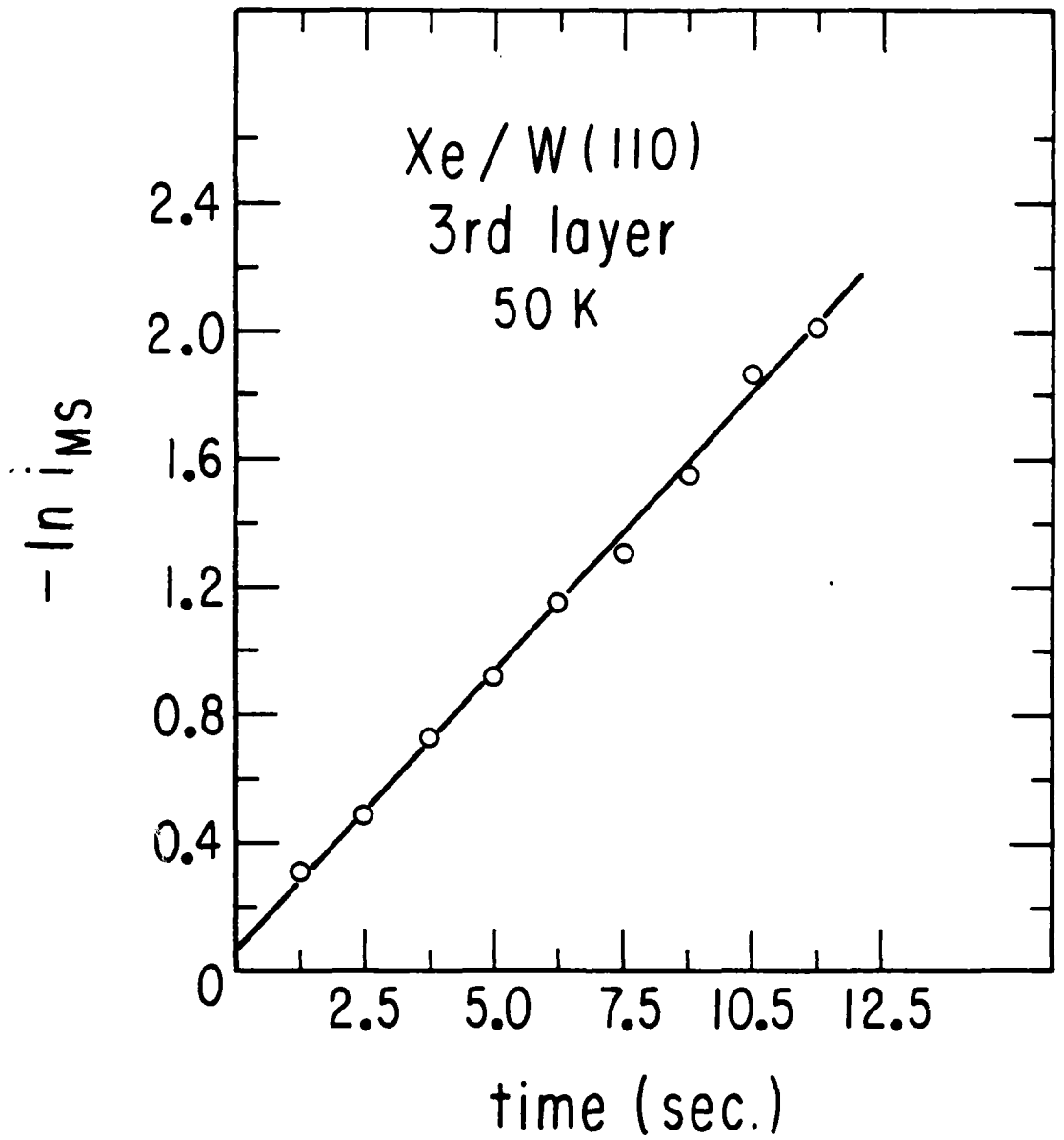


Fig. 9

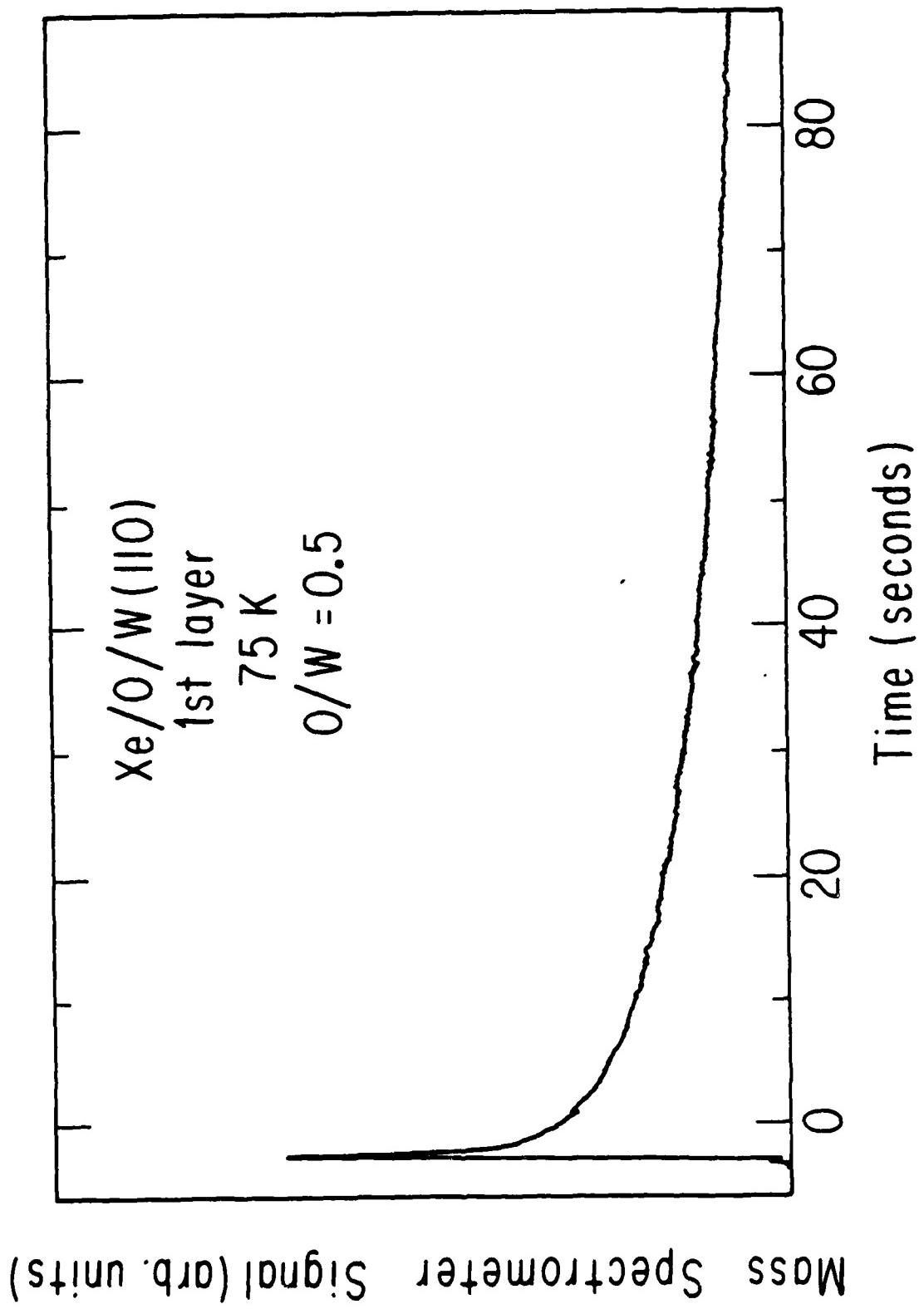


Fig.10

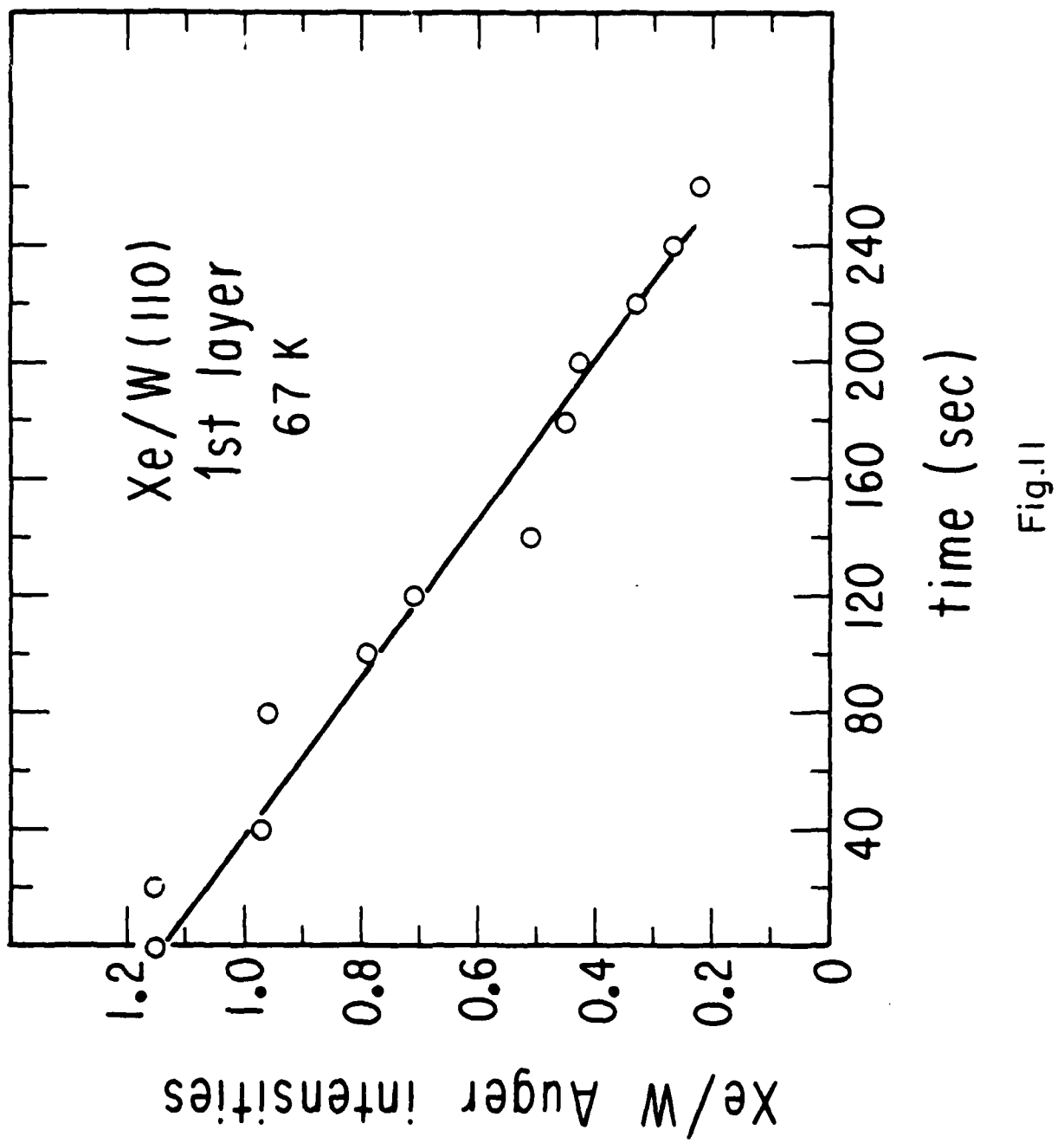


Fig. II

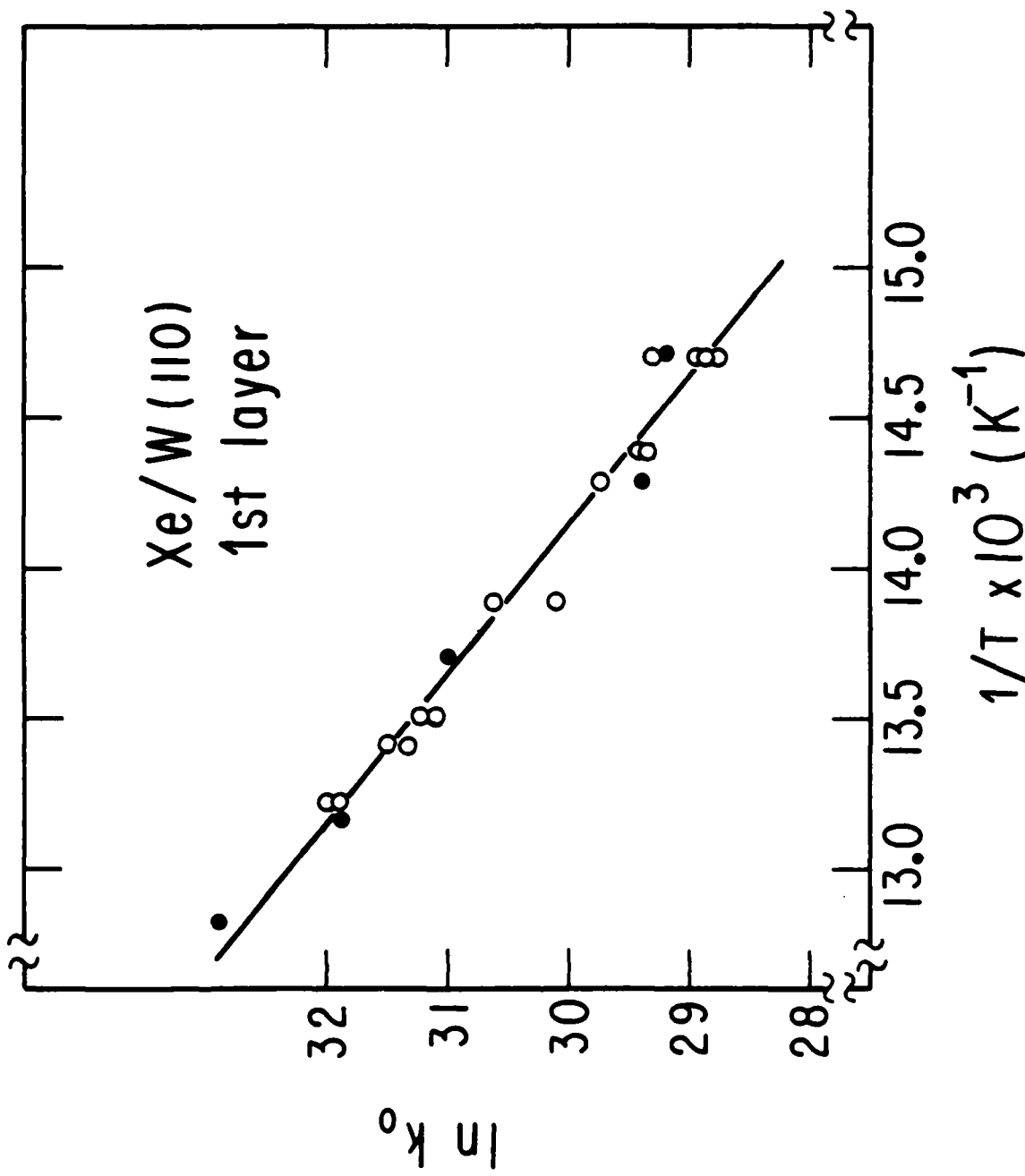


Fig.12

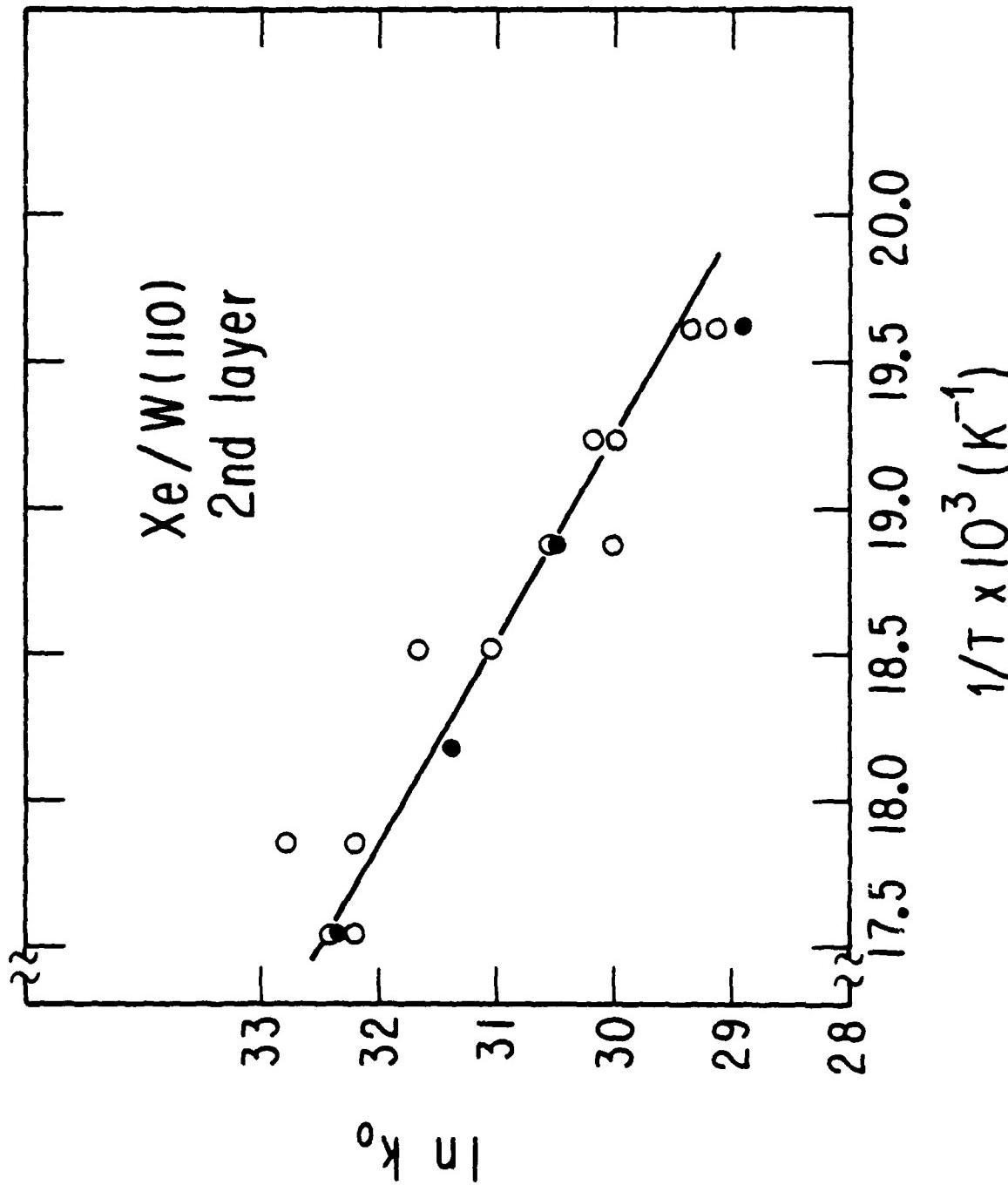


Fig.13

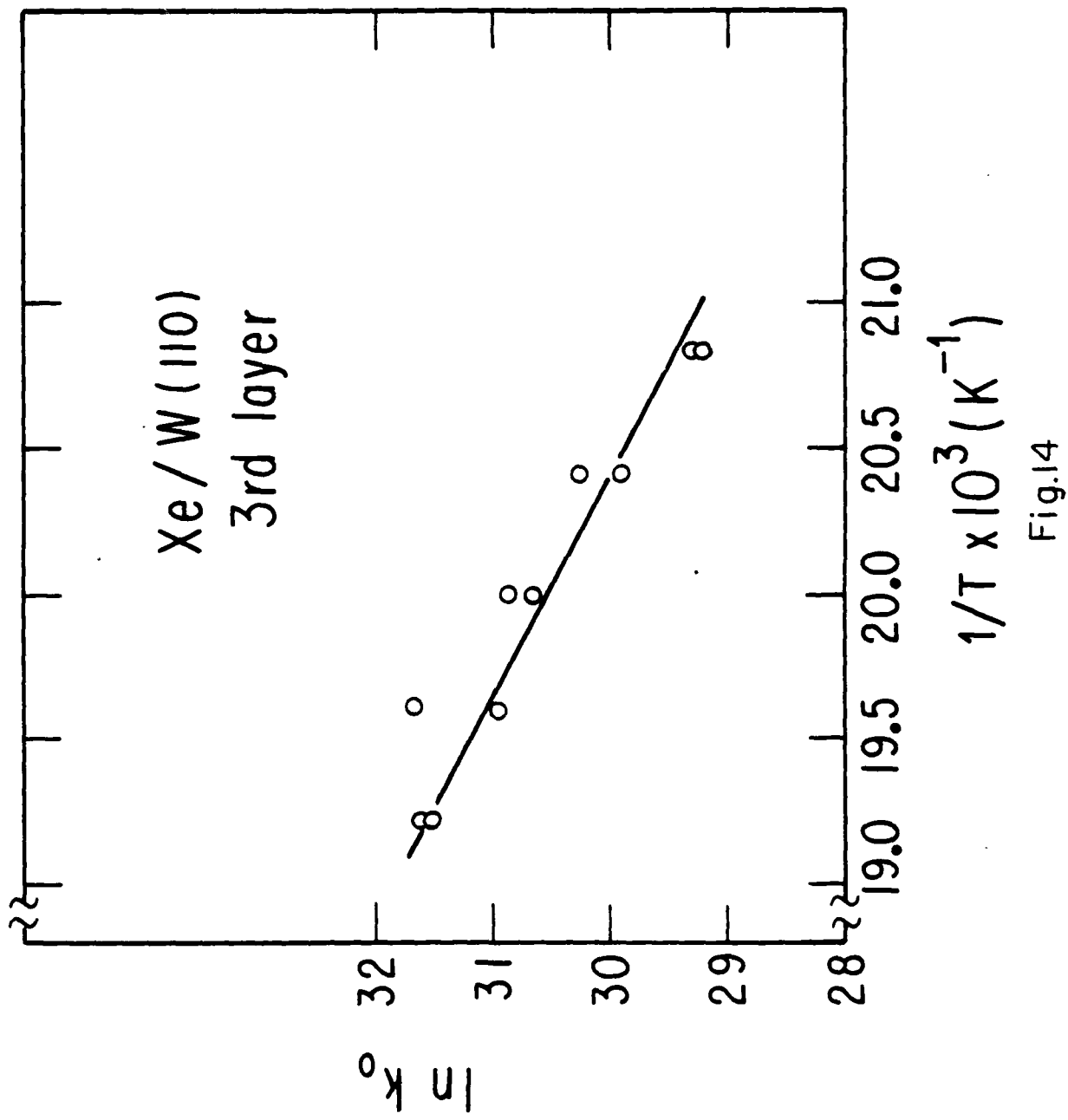


Fig.14

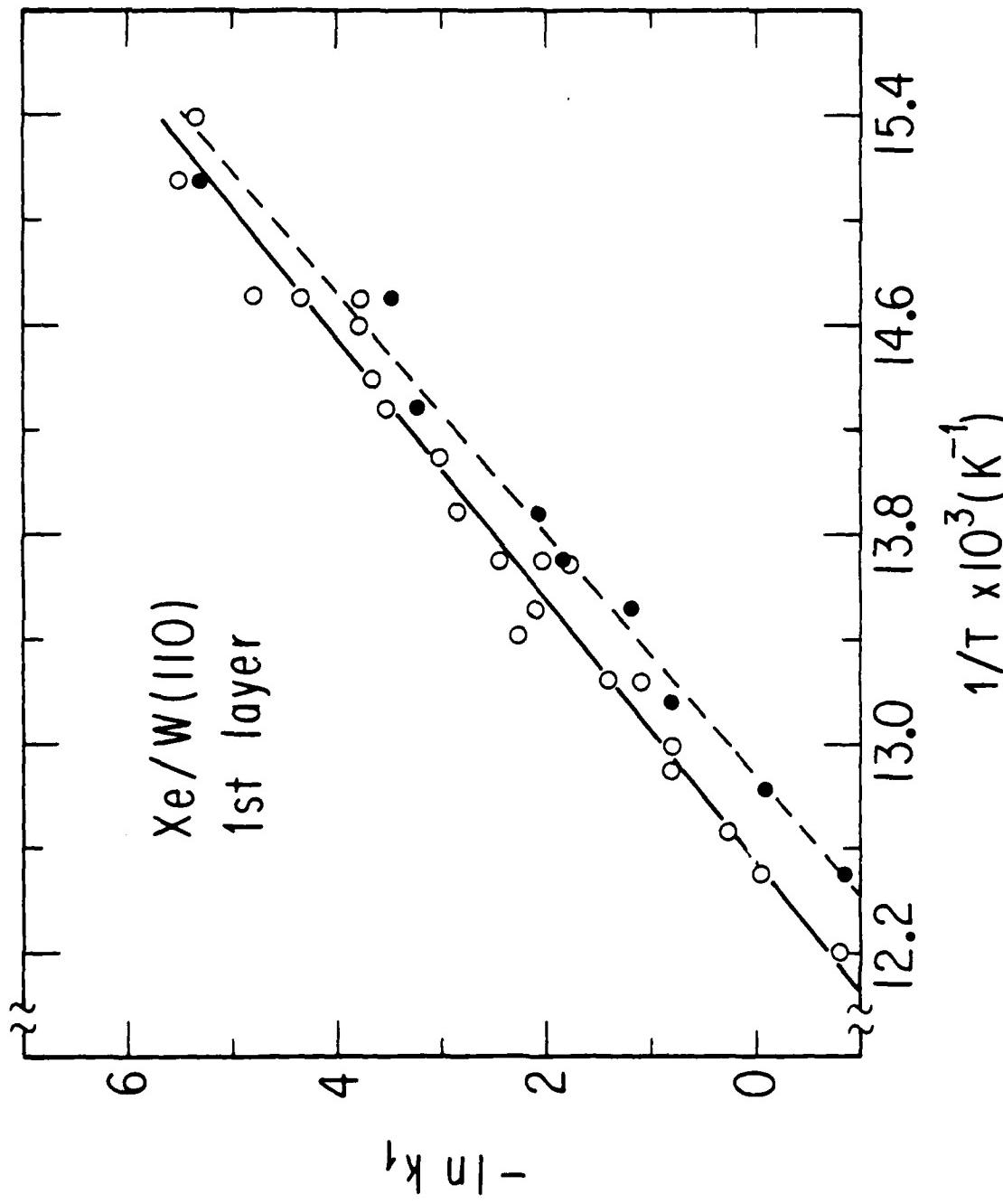


Fig. 15

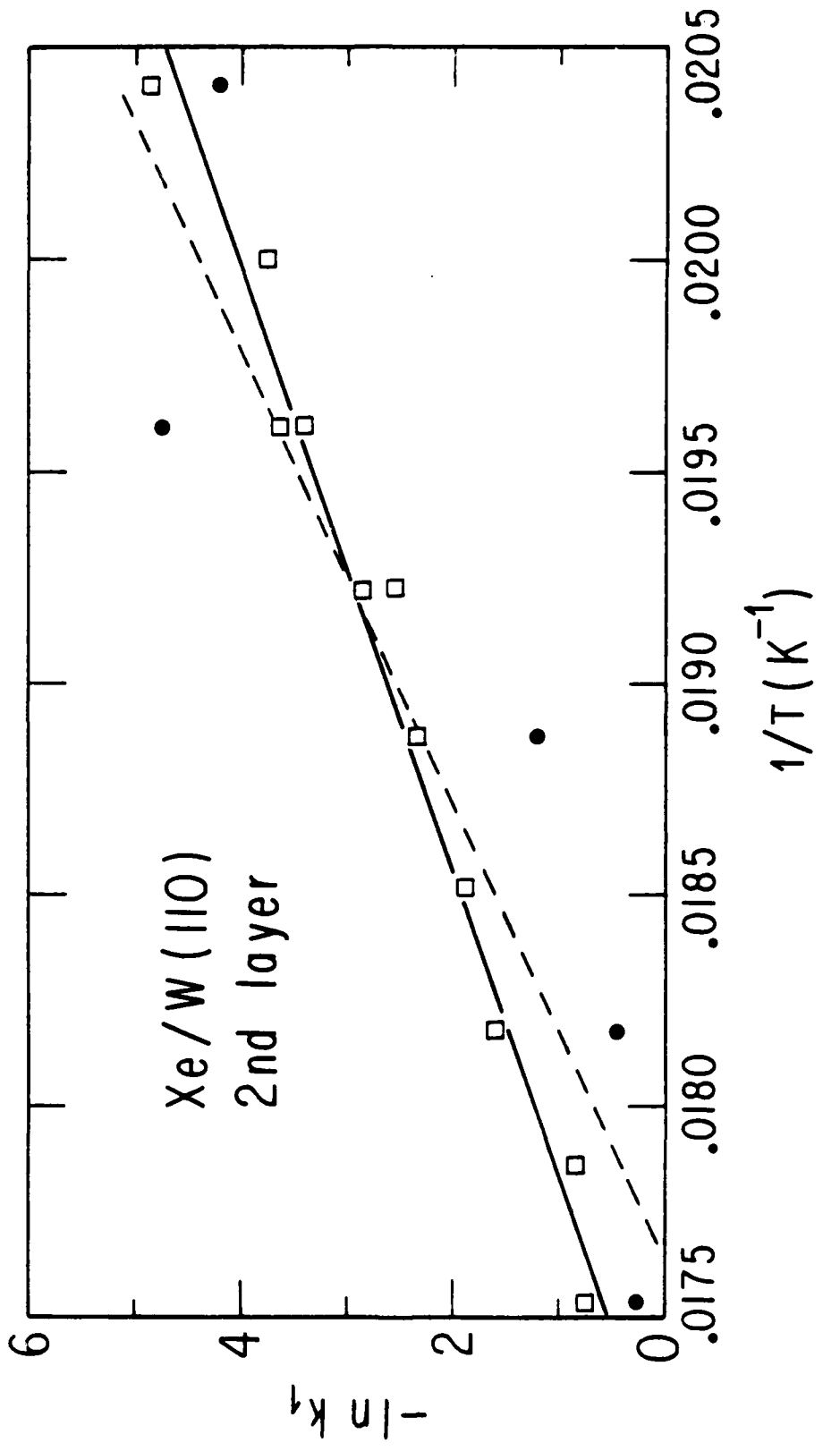


Fig. 16

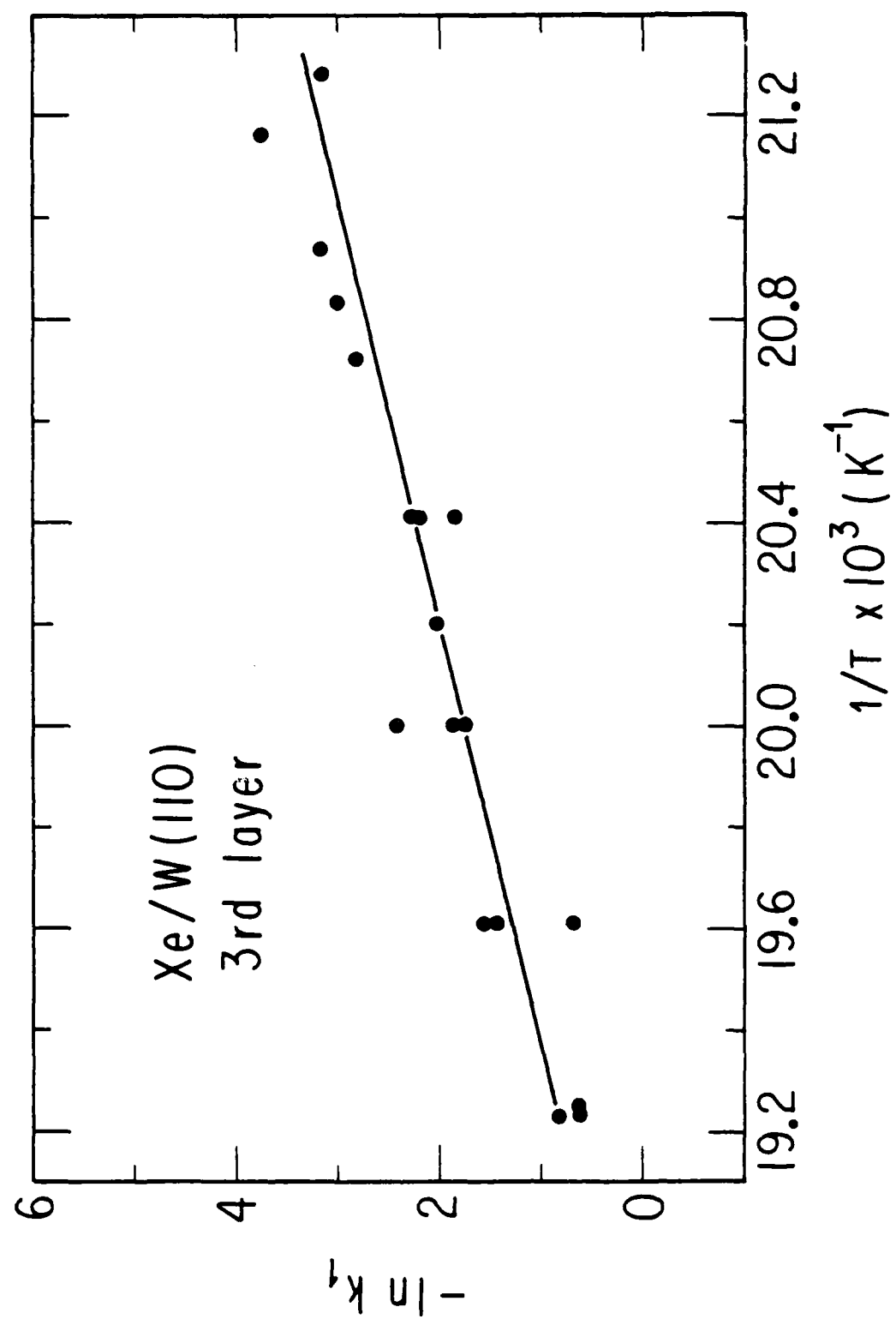


Fig.17

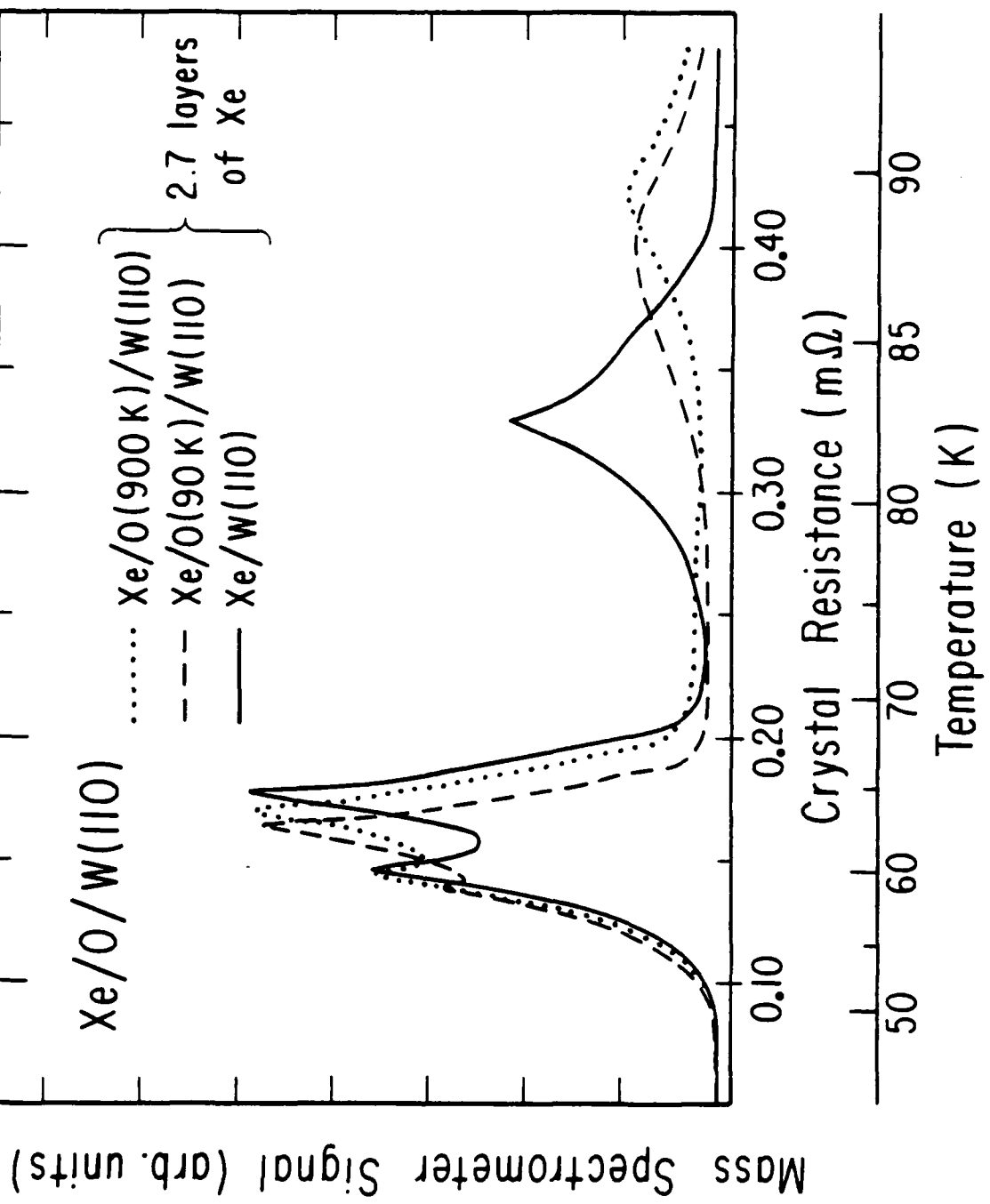


Fig. 18

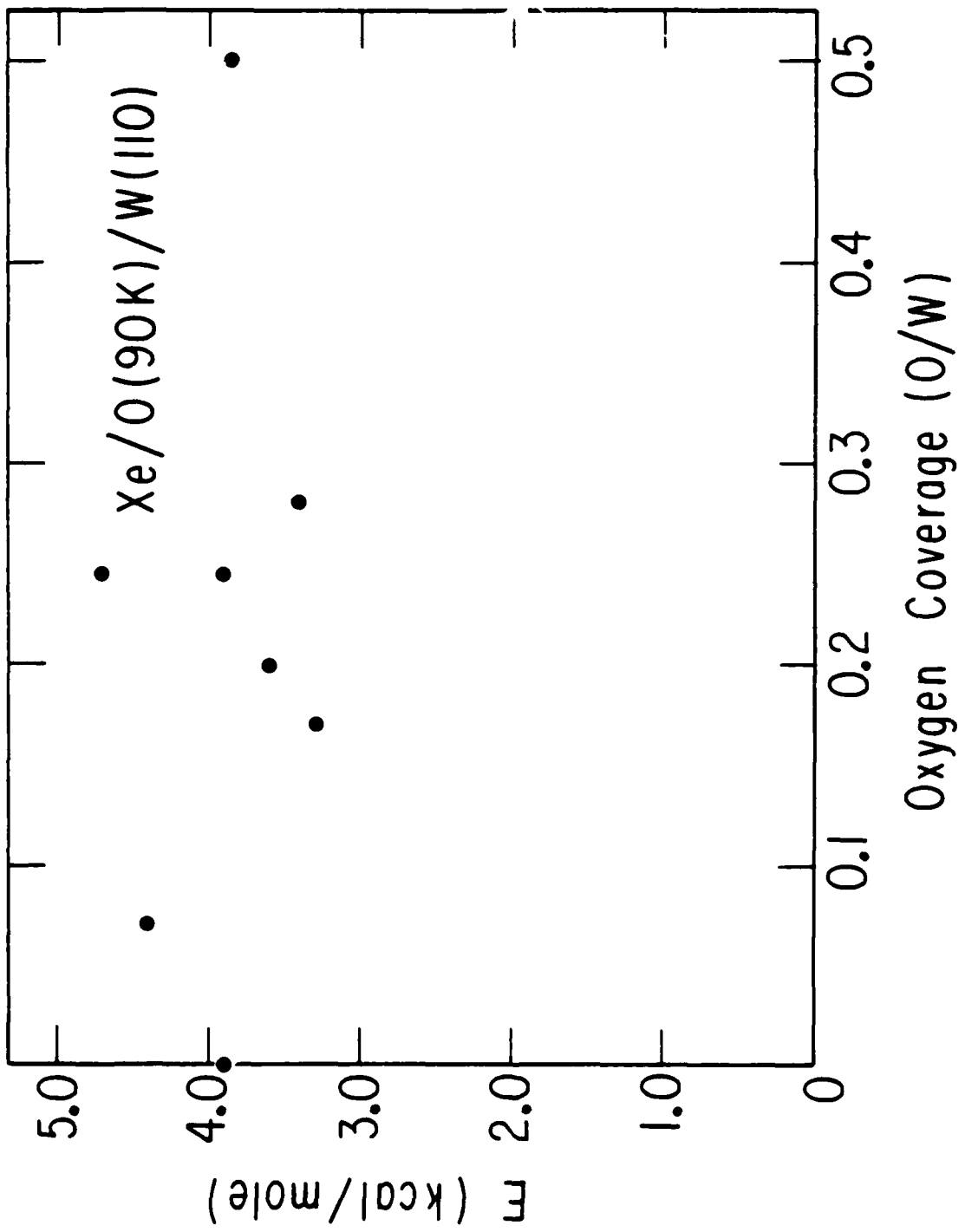


Fig.19

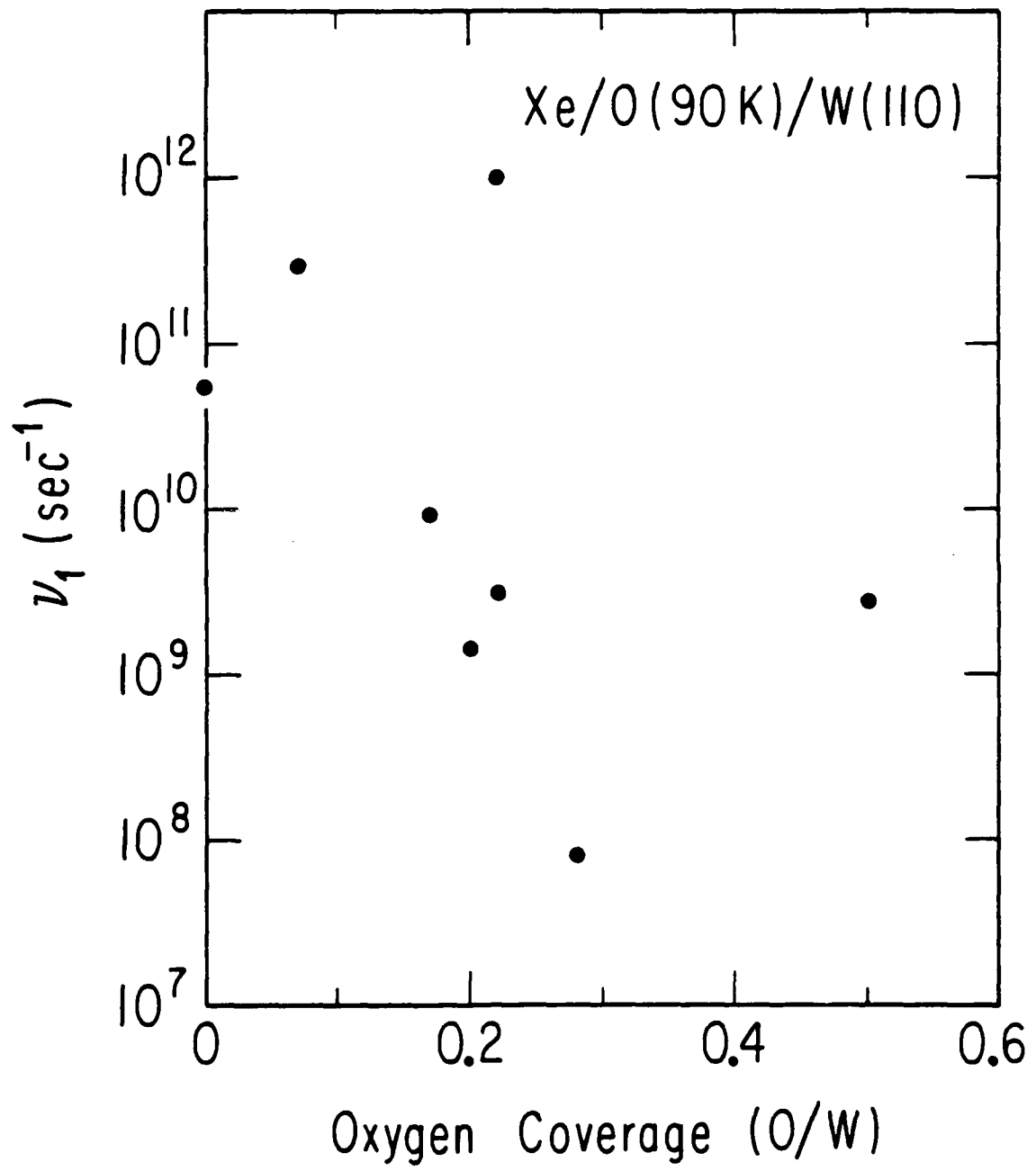
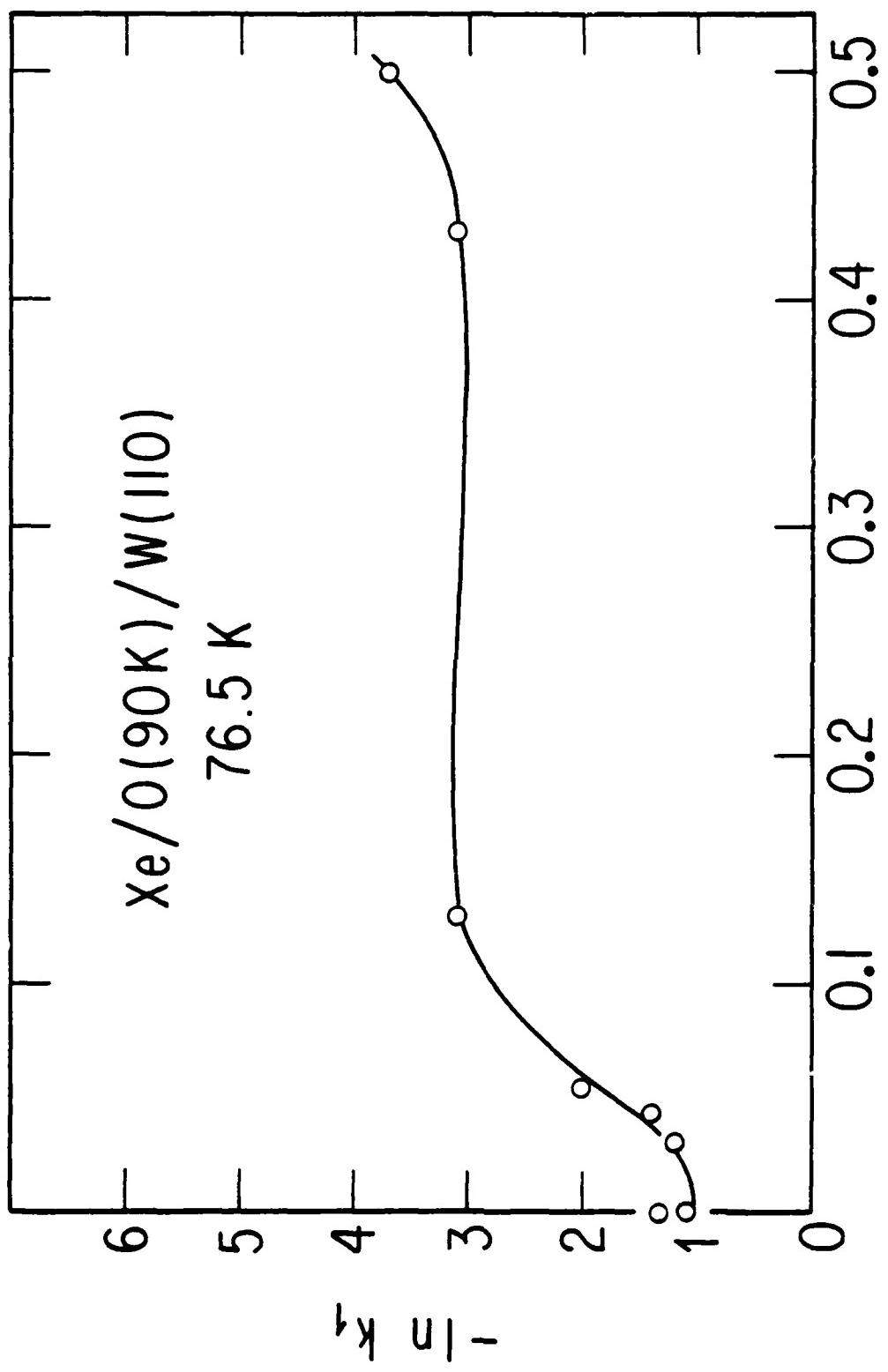


Fig.20

Oxygen Coverage ( $\Theta/W$ )

Fig. 21



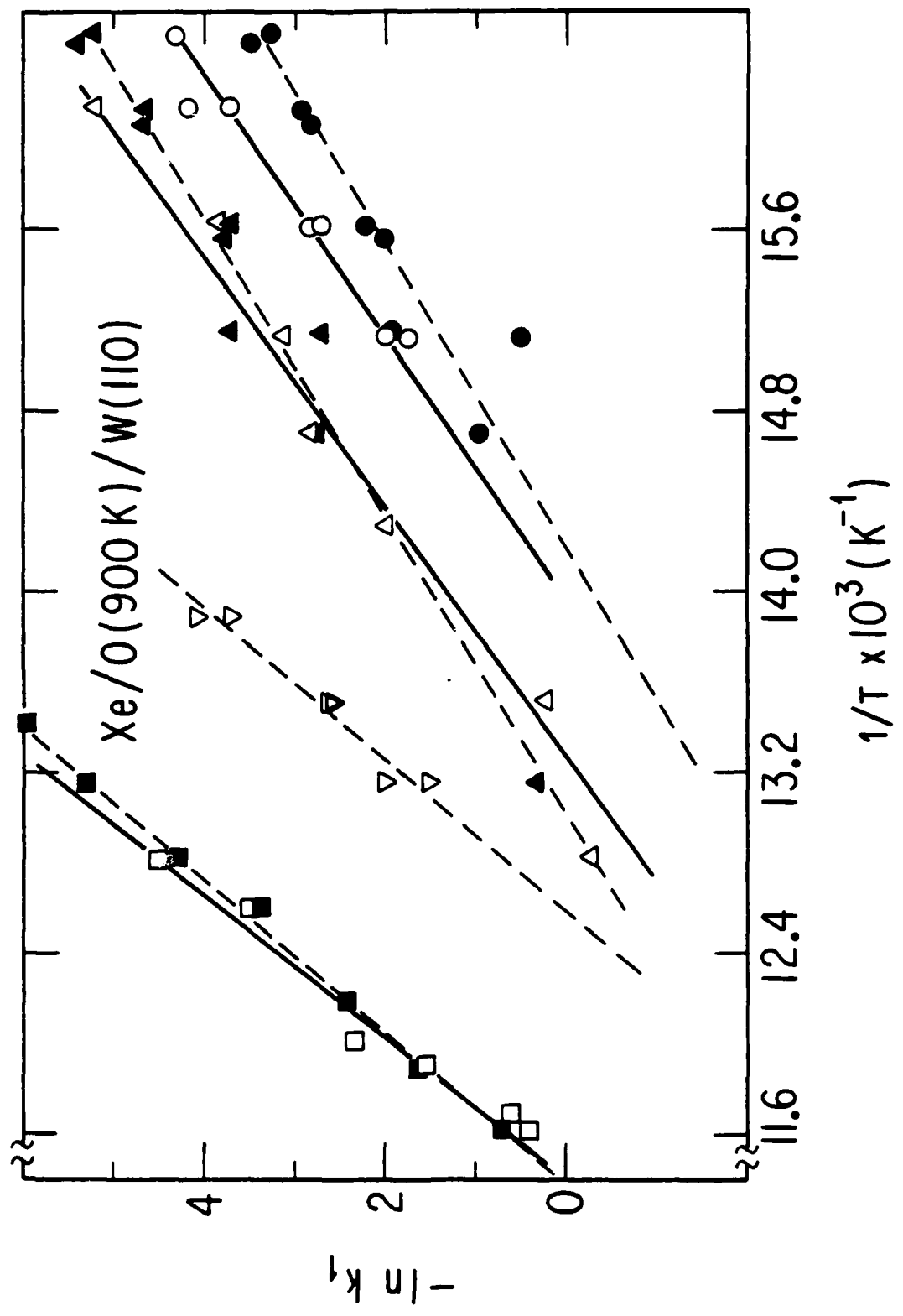


Fig. 22

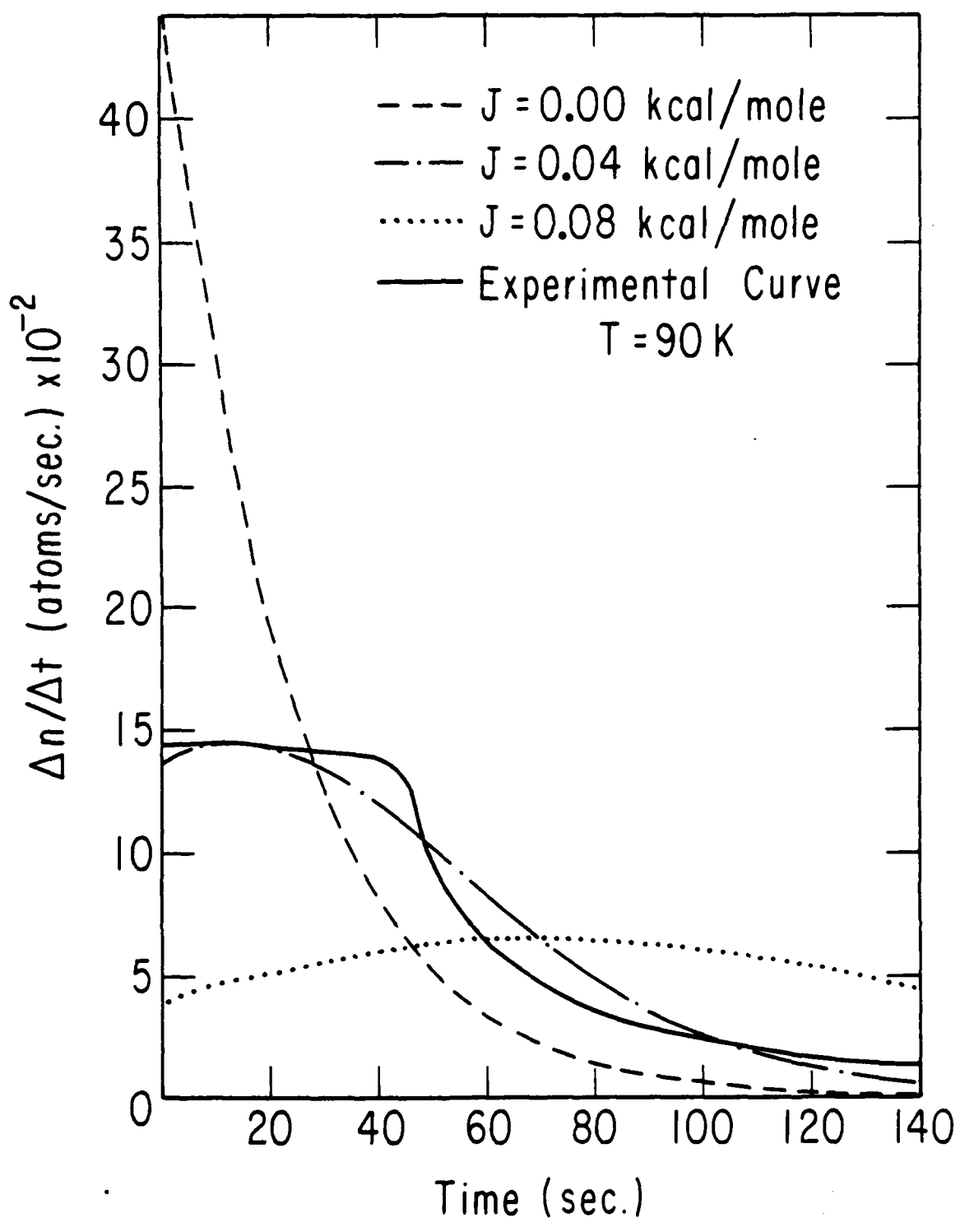


Fig.23

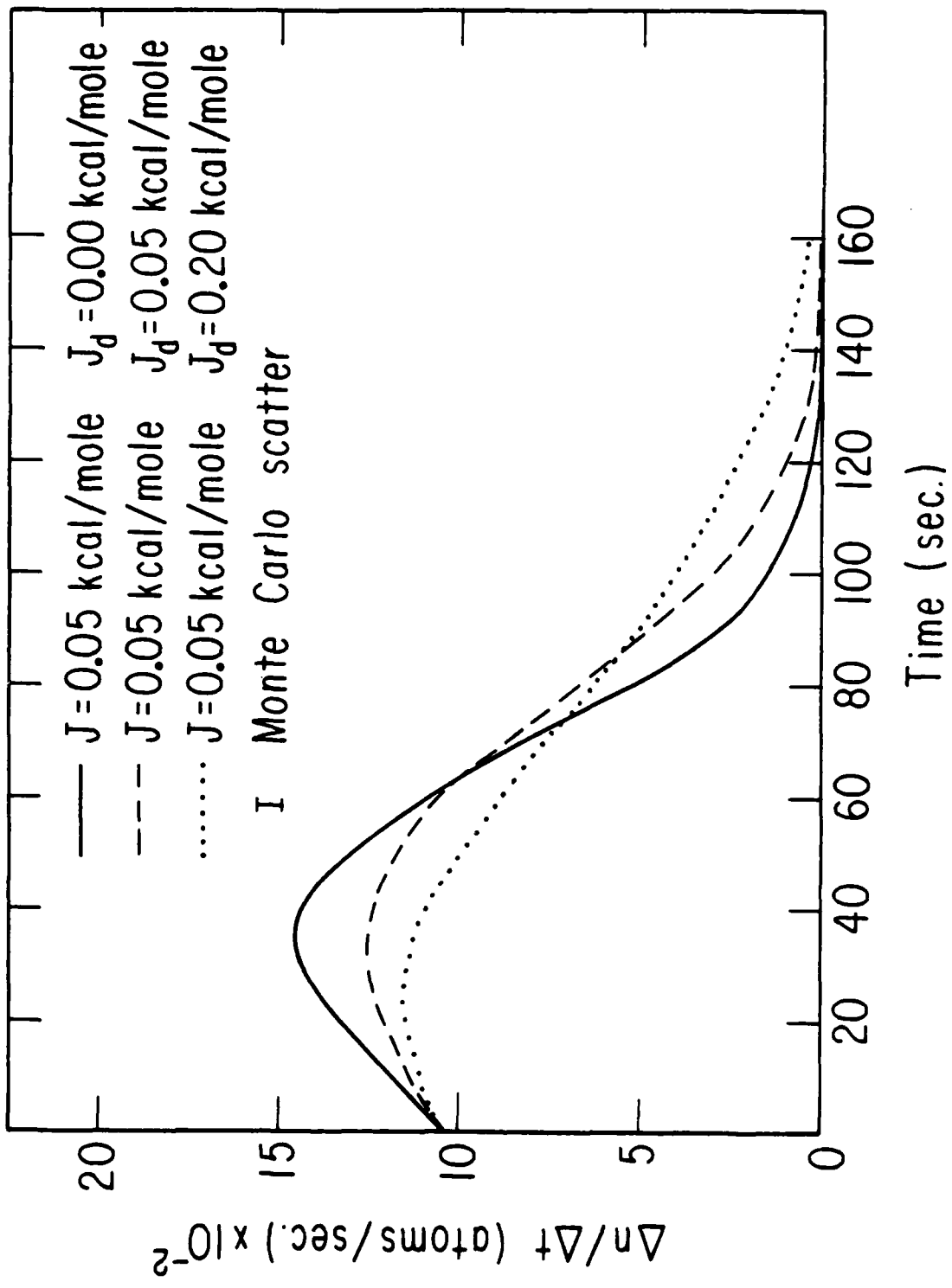


Fig. 24

